

# Second-order quark number susceptibility of deconfined QCD matter in the presence of a magnetic field

Bithika Karmakar,<sup>1,3,\*</sup> Najmul Haque,<sup>2,3,†</sup> and Munshi G Mustafa<sup>1,3,‡</sup>

<sup>1</sup>*Theory Division, Saha Institute of Nuclear Physics,  
1/AF, Bidhannagar, Kolkata 700064, India*

<sup>2</sup>*School of Physical Sciences, National Institute of Science Education and Research,  
Jatni, Khurda 752050, India*

<sup>3</sup>*Homi Bhabha National Institute, Anushaktinagar,  
Mumbai, Maharashtra 400094, India*

Considering the strong field approximation we compute the hard thermal loop pressure at finite temperature and chemical potential of hot and dense deconfined QCD matter in lowest Landau level in one-loop order. We consider the anisotropic pressure in the presence of the strong magnetic field *i.e.*, longitudinal and transverse pressure along parallel and perpendicular to the magnetic field direction. As a first effort we compute and discuss the anisotropic quark number susceptibility of deconfined QCD matter in lowest Landau level. The longitudinal quark number susceptibility is found to increase with the temperature whereas the transverse one decreases with the temperature. We also compute the quark number susceptibility in the weak field approximation. We find that the thermomagnetic correction to the quark number susceptibility is very marginal in the weak field approximation.

---

\* [bithika.karmakar@saha.ac.in](mailto:bithika.karmakar@saha.ac.in)

† [nhaque@niser.ac.in](mailto:nhaque@niser.ac.in)

‡ [munshigolam.mustafa@saha.ac.in](mailto:munshigolam.mustafa@saha.ac.in)

## I. INTRODUCTION

Fluctuations of the conserved quantum numbers like the baryon number, electric charge and strangeness number have been proposed as the probe of a hot and dense matter created in high energy heavy-ion collisions. However if one collects all the charged particles in heavy-ion collision then the net charge will be conserved and there will be no fluctuation. But all the particles can not be collected by any detector [1]. One should consider grand canonical ensemble for the case of real detector. An isolated system does not fluctuate because it is at a thermodynamic limit. But if we consider a small portion of a system which is small enough to consider the rest of the system as a bath and is large enough to ignore the quantum fluctuations then one can calculate the fluctuation of conserved quantities like baryon number using grand canonical ensemble [2]. These fluctuations can be measured experimentally [1–3]. Several lattice calculations are there which calculate fluctuation and correlation of the conserved quantities [4–8]. The fluctuation of the conserved quantum numbers can be used to determine the degrees of freedom of the system [2]. Second- and fourth- order quark number susceptibilities in thermal medium have been calculated using hard-thermal-loop (HTL) approximation [9–14] and perturbative quantum chromodynamics (pQCD) [15–17]. In Ref. [18] the second-order quark number susceptibility (QNS), considering the finite strange-quark mass, was calculated .

On the other hand, recent findings show that the magnetic field of the order of  $10^{18}$  Gauss can be created at the center of the fireball by the charged spectator particles in noncentral heavy-ion collisions [19, 20]. The time-dependent magnetic field is created in a direction perpendicular to the reaction plane [21–25] and its strength depends on the impact parameter. The strength of the magnetic field decreases after few fm/c of the collision [19]. Several activities are under way to study the properties of strongly interacting matter in the presence of a magnetic field. The effects like magnetic catalysis [21, 26, 27], inverse magnetic catalysis [28–36], chiral magnetic effect [37, 38] and meson masses [39–52] in the presence of a magnetic field in noncentral heavy-ion collision have been reported. Furthermore, various thermodynamic quantities [53, 54], transport coefficients [55, 56], dilepton production rate [57–62], photon production rate [63, 64], and damping of photons [65] in a magnetized QCD matter have been obtained.

Here for simplicity, we consider the strong ( $gT < T < \sqrt{|q_f B|}$ ) and weak ( $\sqrt{|q_f B|} < m_{th} \sim gT < T$ ) magnetic field strength with two different scale hierarchies. As a first effort in this article we, using the one-loop HTL pressure of quarks and gluons at finite quark chemical potential in the presence of a magnetic field, calculate the second-order QNS of deconfined QCD matter in these

two scale hierarchies.

The paper is organized as follows: In Sec. II we present the setup to calculate second-order QNS. In Sec. III A, the one-loop HTL free energy of quark in the presence of a strong magnetic field at finite temperature and chemical potential is calculated. The gauge boson free-energy in presence of a strong magnetic field is obtained in Sec. III B. In Sec. III D, we discuss the anisotropic pressure and second-order QNS of the QCD matter in a strong field approximation. Considering the one-loop HTL pressure for the quark-gluon plasma in the weak-field approximation [54], we also calculate and discuss the second-order QNS in the presence of weak magnetic field in Sec. IV. We conclude in Sec. V.

## II. SETUP

Here we consider the deconfined QCD matter as a grand canonical ensemble.

The free energy of the system is given by

$$\mathcal{F}(T, V, \mu) = U - TS - \mu N \quad (1)$$

where  $\mu$  is the quark chemical potential and  $U$ ,  $N$ , and  $S$  are the total energy, net quark number, and entropy of the system, respectively. Hence, the free energy density or the thermodynamic potential of the system can be written as

$$F = \mathcal{F}/V = u - Ts - \mu n \quad (2)$$

where  $u$ ,  $n$ , and  $s$  are the total energy density, net quark number density, and entropy density of the system, respectively. The pressure of the system is given as

$$P = -F. \quad (3)$$

However, we consider the system to be anisotropic in the presence of a strong magnetic field and the free energy of the system is defined in Sec. III.

Now, the second-order QNS is defined as

$$\chi = -\frac{\partial^2 F}{\partial \mu^2} \Big|_{\mu=0} = \frac{\partial^2 P}{\partial \mu^2} \Big|_{\mu=0} = \frac{\partial n}{\partial \mu} \Big|_{\mu=0}, \quad (4)$$

which is the measure of the variance or the fluctuation of the net quark number. One can find out the covariance of two conserved quantities when the quark flavors have different chemical potential. Alternatively, one can work with other bases according to the system e.g., the net baryon number  $\mathcal{B}$ , net charge  $\mathcal{Q}$  and strangeness number  $\mathcal{S}$  or  $\mathcal{B}$ ,  $\mathcal{Q}$  and third-component of the

isospin  $\mathcal{I}_3$ . In our case we take the strangeness and charge chemical potential to be zero. Moreover, we consider same chemical potential for all flavors which results the vanishing off-diagonal quark number susceptibilities. Thus the net second-order baryon number susceptibility is related to the second-order QNS as  $\chi_B = \frac{1}{3}\chi$ .

The strength of the magnetic field produced in a noncentral heavy-ion collision can be up to  $(10 - 20)m_\pi^2$  at the time of the collision [66]. However, it decreases very fast being inversely proportional to the square of time [63, 67]. But if one considers finite electric conductivity of the medium, then the magnetic field strength will not die out very fast [61, 68–74]. We consider two different cases with strong and weak magnetic field in this article.

### III. STRONG MAGNETIC FIELD

In this section we consider the strong field scale hierarchy  $gT < T < \sqrt{eB}$ . In the presence of the magnetic field, the energy of charged fermion becomes  $E_n = \sqrt{k_3^2 + m_f^2 + 2nq_f B}$  where  $k_3$  is the momentum of a fermion along the magnetic field direction,  $m_f$  is the mass of the fermion and the Landau level,  $n$ , can vary from 0 to  $\infty$ . The transverse momentum of the fermion becomes quantized. It can be shown that at very high value of the magnetic field, the contribution from all the Landau levels, except the lowest Landau level, can be ignored [58]. Consequently, the dynamics becomes  $(1 + 1)$  dimensional when one considers only the lowest Landau level (LLL). The general structures of the quark and gluon self-energy in the presence of the magnetic field have been formulated in Ref. [53] at finite temperature but for zero quark chemical potential. Here we extend it for the case of nonzero quark chemical potential. In the presence of the strong magnetic field, the general structure of quark self-energy can be written from Ref [53] as

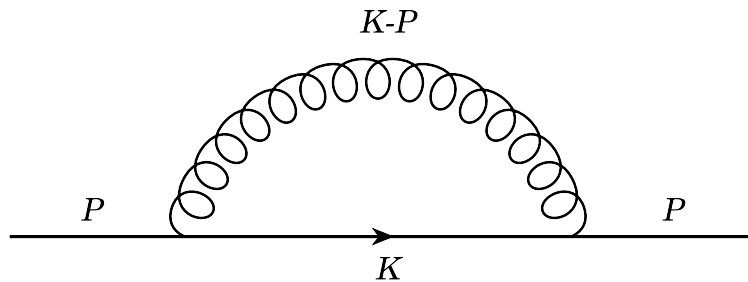


FIG. 1: Quark self-energy diagram

$$\Sigma(p_0, p_3) = a\not{p} + b\not{p} + c\gamma_5\not{p} + d\gamma_5\not{p}, \quad (5)$$

where the rest frame of heat bath velocity is  $u_\mu = (1, 0, 0, 0)$  and the direction of magnetic field is  $n_\mu = (0, 0, 0, 1)$ . Now, the various form factors can be obtained as

$$a = \frac{1}{4} \text{Tr}[\Sigma \not{n}], \quad (6)$$

$$b = -\frac{1}{4} \text{Tr}[\Sigma \not{p}], \quad (7)$$

$$c = \frac{1}{4} \text{Tr}[\gamma_5 \Sigma \not{n}], \quad (8)$$

$$d = -\frac{1}{4} \text{Tr}[\gamma_5 \Sigma \not{p}]. \quad (9)$$

Considering Fig. 1 the above form factors are calculated up to  $\mathcal{O}[(\mu/T)^4]$  in Appendix A as

$$a = -d = c_1 \left[ \frac{p_0}{p_0^2 - p_3^2} c_2 + \frac{(p_0^2 + p_3^2)}{2(p_0^2 - p_3^2)^2} c_3 \right], \quad (10)$$

$$b = -c = -c_1 \left[ \frac{p_3}{p_0^2 - p_3^2} c_2 + \frac{p_0 p_3}{(p_0^2 - p_3^2)^2} c_3 \right], \quad (11)$$

where  $c_1, c_2$ , and  $c_3$  are defined in Eqs. (A10).

### A. One-loop quark free energy in the presence of a strongly magnetized medium

In this section we calculate the quark free energy within the HTL approximation using the form factors of quark self-energy in (10) and (11). The quark free energy can be written as

$$F_q = -d_F \oint_{\{p_0\}} \frac{d^3 p}{(2\pi)^3} \ln (\det[S_{\text{eff}}^{-1}(p_0, p_3)]), \quad (12)$$

where  $d_F = N_c N_f$ . Here we use the sum-integral as

$$\oint_{\{p_0\}} \equiv T \sum_{p_0=(2n+1)\pi iT+\mu} \int \frac{d^3 p}{(2\pi)^3}. \quad (13)$$

The inverse of the effective fermion propagator can be written as

$$\begin{aligned} S_{\text{eff}}^{-1} &= \not{p} + \Sigma = (p_0 + a)\not{n} + (b - p_3)\not{p} + c\gamma_5 \not{n} + d\gamma_5 \not{p} \\ &= (p_0 + a)\gamma^0 + (b - p_3)\gamma^3 + c\gamma_5 \gamma^0 + d\gamma_5 \gamma^3. \end{aligned} \quad (14)$$

Now we evaluate the determinant as

$$\begin{aligned} \det[S_{\text{eff}}^{-1}] &= \left( (b + c - p_3)^2 - (a + d + p_0)^2 \right) \left( (-b + c + p_3)^2 - (a - d + p_0)^2 \right) \\ &= (p_0^2 - p_3^2) \left( (p_0 + 2a)^2 - (p_3 - 2b)^2 \right) \\ &= P_{||}^2 (P_{||}^2 + 4ap_0 + 4bp_3 + 4a^2 - 4b^2) \end{aligned}$$

$$= P_{||}^4 \left( 1 + \frac{4a^2 - 4b^2 + 4ap_0 + 4bp_3}{P_{||}^2} \right), \quad (15)$$

where we have used  $d = -a$  and  $c = -b$ .

So Eq. (12) becomes

$$\begin{aligned} F_q &= -d_F \sum_{\{p_0\}} \frac{d^3 p}{(2\pi)^3} \ln \left[ P_{||}^4 \left( 1 + \frac{4a^2 - 4b^2 + 4ap_0 + 4bp_3}{P_{||}^2} \right) \right] \\ &= -2d_F \sum_{\{p_0\}} \frac{d^3 p}{(2\pi)^3} \ln(-P_{||}^2) - d_F \sum_{\{p_0\}} \frac{d^3 p}{(2\pi)^3} \ln \left[ 1 + \frac{4a^2 - 4b^2 + 4ap_0 + 4bp_3}{P_{||}^2} \right] \\ &= F_q^{\text{ideal}} + F'_q, \end{aligned} \quad (16)$$

where the free energy of free quarks in the presence of a magnetic field [75] reads as

$$\begin{aligned} F_q^{\text{ideal}} &= -2d_F \sum_{\{p_0\}} \frac{d^3 p}{(2\pi)^3} \ln(-P_{||}^2) = -2d_F \sum_f \frac{q_f B}{(2\pi)^2} \sum_{\{p_0\}} dp_3 \ln(-P_{||}^2) \\ &= -d_F \sum_f \frac{q_f B T^2}{6} \left( 1 + 12\hat{\mu}^2 \right), \end{aligned} \quad (17)$$

where  $\hat{\mu} = \mu/2\pi T$ , and

$$\begin{aligned} F'_q &= -d_F \sum_{\{p_0\}} \frac{d^3 p}{(2\pi)^3} \ln \left[ 1 + \frac{4a^2 - 4b^2 + 4ap_0 + 4bp_3}{P_{||}^2} \right] \\ &= -d_F \sum_{\{p_0\}} \frac{d^3 p}{(2\pi)^3} \left[ \frac{4(ap_0 + bp_3)}{P_{||}^2} + \frac{4(a^2 P_{||}^2 - b^2 P_{||}^2 - 2a^2 p_0^2 - 2b^2 p_3^2 - 4abp_0 p_3)}{P_{||}^4} \right. \\ &\quad \left. + \mathcal{O}(g^6) \right], \end{aligned} \quad (18)$$

where we have kept terms up to  $\mathcal{O}(g^4)$  to obtain the analytic expression of free energy. The expansion made above is valid for  $g^2(q_f B/T^2) < 1$ , which can be realized as  $(q_f B)/T^2 \gtrsim 1$  and  $g \ll 1$ .

As the fermions are considered to be in LLL in the strong field approximation, Eq. (18) becomes

$$\begin{aligned} F'_q &= -d_F \sum_f \frac{q_f B}{(2\pi)^2} \sum_{\{p_0\}} dp_3 \left[ \frac{4(ap_0 + bp_3)}{P_{||}^2} + \frac{4(a^2 P_{||}^2 - b^2 P_{||}^2 - 2a^2 p_0^2 - 2b^2 p_3^2 - 4abp_0 p_3)}{P_{||}^4} \right. \\ &\quad \left. + \mathcal{O}(g^6) \right]. \end{aligned} \quad (19)$$

The sum-integrals are calculated in Appendix B and the expression for the quark free energy up to  $\mathcal{O}(g^4)$  is obtained by adding individual contributions as

$$F_q = F_q^{\text{ideal}} + F'_q = -d_F \sum_f \frac{q_f B T^2}{6} \left( 1 + \frac{3\mu^2}{4\pi^2 T^2} \right) \quad (20)$$

$$\begin{aligned}
& + 4d_F \sum_f \frac{g^2 C_F(q_f B)^2}{(2\pi)^4} \left( \frac{\Lambda}{4\pi T} \right)^{2\epsilon} \left[ \frac{1}{\epsilon} \left( -\frac{1}{2} \ln 2 + \frac{7\mu^2 \zeta(3)}{16\pi^2 T^2} - \frac{31\mu^4 \zeta(5)}{64\pi^4 T^4} \right) - \frac{3\gamma_E \ln 2}{2} \right. \\
& + \ln 2 \ln \pi - \frac{1}{2} \ln 2 \ln 16\pi + \frac{g^2 C_F(q_f B)}{4\pi^2} \frac{63 \ln 2^2 \zeta(3)}{72\pi^2 T^2} - \frac{g^2 C_F(q_f B)}{4\pi^2} \frac{217(q_f B)^2 \zeta(5)}{36864\pi^4 T^6} \\
& \times \left( \gamma_E + 2 \ln 2 - 12 \ln G \right)^2 + \frac{\mu^2}{1152\pi^2 T^4} \left\{ \frac{7\zeta(3)g^2 C_F(q_f B)}{4\pi^2} \left( 3 + 3\gamma_E + 4 \ln 2 - 36 \ln G \right)^2 \right. \\
& + 504T^2 \zeta(3) \left( 3\gamma_E + 8 \ln 2 - \ln \pi \right) - \frac{36 \ln 2}{\pi^2} \frac{g^2 C_F(q_f B)}{4\pi^2} \left( 49\zeta(3)^2 + 186 \ln 2 \zeta(5) \right) \Big\} \\
& - \frac{7(q_f B)^2 \mu^2}{737280\pi^4 T^8} \frac{g^2 C_F(q_f B)}{4\pi^2} \left\{ -31\zeta(5) \left( -15 + 15\gamma_E + 16 \ln 2 \right) \left( \gamma_E + 2 \ln 2 - 12 \ln G \right) \right. \\
& - \frac{48825}{\pi^4} \zeta(3)^2 \zeta(5) - \frac{9525\zeta(7)}{\pi^2} \left( \gamma_E + 2 \ln 2 - 12 \ln G \right)^2 + 55800\zeta(5)\zeta'(-3) \\
& \times \left( \gamma_E + 2 \ln 2 - 12 \ln G \right) \Big\} + \frac{\mu^4}{69120\pi^6 T^6} \left\{ -1080\pi^2 T^2 \left( 98\zeta(3)^2 + 31\zeta(5) \left( 3\gamma_E + 8 \ln 2 - \ln \pi \right) \right) \right. \\
& - \frac{g^2 C_F(q_f B)}{4\pi^2} \left( 14\pi^4 \zeta(3) \left( 15\gamma_E + 16 \ln 2 \right) \left( 3 + 3\gamma_E + 4 \ln 2 - 36 \ln G \right) - 46305\zeta(3)^3 \right. \\
& + 2790\pi^2 \zeta(5) \left( 3 + 3\gamma_E - 4 \ln 2 - 36 \ln G \right)^2 - 820260 \ln 2 \zeta(3) \zeta(5) - 1028700 \ln 2^2 \zeta(7) \\
& - 25200\pi^4 \zeta(3) \zeta'(-3) \left( 3 + 3\gamma_E + 4 \ln 2 - 36 \ln G \right) \Big\} - \frac{\mu^4 (q_f B)^2}{5308416\pi^4 T^{10}} \frac{g^2 C_F(q_f B)}{4\pi^2} \\
& \times \left\{ \frac{10897740}{\pi^6} \zeta(3) \zeta(5)^2 + \frac{37804725}{\pi^6} \zeta(3)^2 \zeta(7) + \frac{2253510\zeta(9)}{\pi^4} \left( \gamma_E + 2 \ln 2 - 12 \ln G \right)^2 \right. \\
& + \frac{24003}{\pi^2} \zeta(7) \left( \gamma_E + 2 \ln 2 - 12 \ln G \right) \left( -15 + 15\gamma_E + 16 \ln 2 - 1800\zeta'(-3) \right) \\
& + \frac{31\zeta(5)}{100} \left( 14175 - 40950\gamma_E + 26775\gamma_E^2 + 68240\gamma_E \ln 2 + 41728 \ln 2^2 + 151200 \ln G \right. \\
& - 151200\gamma_E \ln G - 240 \ln 2 \left( 231 + 640 \ln G \right) + 3175200\zeta'(-5) \left( \gamma_E + 2 \ln 2 - 12 \ln G \right) \\
& \left. \left. - 226800\zeta'(-3) \left( -15 + 15\gamma_E + 16 \ln 2 \right) + 204120000\zeta'(-3)^2 \right) \right\} \Bigg]. \tag{21}
\end{aligned}$$

The divergences are regulated by adding suitable counterterms as

$$F_{ct} = -4d_F \sum_f \frac{g^2 C_F(q_f B)^2}{(4\pi^2)^2} \left[ -\frac{1}{2\epsilon} \left( \ln 2 - \frac{7}{8\pi^2} \frac{\mu^2}{T^2} \zeta(3) + \frac{31}{24} \frac{\mu^4}{T^4} \frac{3}{4\pi^4} \zeta(5) \right) \right]. \tag{22}$$

The renormalized quark free-energy is given as

$$\begin{aligned}
F_q^r & = -d_F \sum_f \frac{q_f B T^2}{6} \left( 1 + 12\hat{\mu}^2 \right) + 4d_F \sum_f \frac{g^2 C_F(q_f B)^2}{(2\pi)^4} \left[ -\ln 2 \ln \frac{\hat{\Lambda}}{2} - \frac{3\gamma_E \ln 2}{2} \right. \\
& + \ln 2 \ln \pi - \frac{1}{2} \ln 2 \ln 16\pi + \frac{g^2 C_F(q_f B)}{4\pi^2} \frac{63 \ln 2^2 \zeta(3)}{72\pi^2 T^2} - \frac{g^2 C_F(q_f B)}{4\pi^2} \frac{217(q_f B)^2 \zeta(5)}{36864\pi^4 T^6} \\
& \times \left( \gamma_E + 2 \ln 2 - 12 \ln G \right)^2 + \frac{7\hat{\mu}^2}{2} \zeta(3) \ln \frac{\hat{\Lambda}}{2} + \frac{\hat{\mu}^2}{288T^2} \left\{ \frac{7\zeta(3)g^2 C_F(q_f B)}{4\pi^2} \right. \\
& \times \left( 3 + 3\gamma_E + 4 \ln 2 - 36 \ln G \right)^2 + 504T^2 \zeta(3) \left( 3\gamma_E + 8 \ln 2 - \ln \pi \right) - \frac{36 \ln 2}{\pi^2} \frac{g^2 C_F(q_f B)}{4\pi^2}
\end{aligned}$$

$$\begin{aligned}
& \times \left( 49\zeta(3)^2 + 186 \ln 2 \zeta(5) \right) \Bigg\} - \frac{7(q_f B)^2 \hat{\mu}^2}{184320 \pi^2 T^6} \frac{g^2 C_F(q_f B)}{4\pi^2} \left\{ -31\zeta(5) \left( -15 + 15\gamma_E + 16 \ln 2 \right) \right. \\
& \times \left( \gamma_E + 2 \ln 2 - 12 \ln G \right) - \frac{48825}{\pi^4} \zeta(3)^2 \zeta(5) - \frac{9525 \zeta(7)}{\pi^2} \left( \gamma_E + 2 \ln 2 - 12 \ln G \right)^2 \\
& + 55800 \zeta(5) \zeta'(-3) \left( \gamma_E + 2 \ln 2 - 12 \ln G \right) \Bigg\} - \frac{31 \hat{\mu}^4}{2} \zeta(5) \ln \frac{\hat{\Lambda}}{2} + \frac{\hat{\mu}^4}{4320 \pi^2 T^2} \left\{ -1080 \pi^2 T^2 \right. \\
& \times \left( 98 \zeta(3)^2 + 31 \zeta(5) \left( 3\gamma_E + 8 \ln 2 - \ln \pi \right) \right) - \frac{g^2 C_F(q_f B)}{4\pi^2} \left( 14 \pi^4 \zeta(3) \left( 15\gamma_E + 16 \ln 2 \right) \right. \\
& \times \left( 3 + 3\gamma_E + 4 \ln 2 - 36 \ln G \right) - 46305 \zeta(3)^3 + 2790 \pi^2 \zeta(5) \left( 3 + 3\gamma_E - 4 \ln 2 - 36 \ln G \right)^2 \\
& - 820260 \ln 2 \zeta(3) \zeta(5) - 1028700 \ln^2 \zeta(7) - 25200 \pi^4 \zeta(3) \zeta'(-3) \left( 3 + 3\gamma_E + 4 \ln 2 - 36 \ln G \right) \Bigg\} \\
& - \frac{\hat{\mu}^4 (q_f B)^2}{331776 T^6} \frac{g^2 C_F(q_f B)}{4\pi^2} \left\{ \frac{10897740}{\pi^6} \zeta(3) \zeta(5)^2 + \frac{37804725}{\pi^6} \zeta(3)^2 \zeta(7) + \frac{2253510 \zeta(9)}{\pi^4} \right. \\
& \times \left( \gamma_E + 2 \ln 2 - 12 \ln G \right)^2 + \frac{24003}{\pi^2} \zeta(7) \left( \gamma_E + 2 \ln 2 - 12 \ln G \right) \left( -15 + 15\gamma_E + 16 \ln 2 \right. \\
& - 1800 \zeta'(-3) \Bigg) + \frac{31 \zeta(5)}{100} \left( 14175 - 40950 \gamma_E + 26775 \gamma_E^2 + 68240 \gamma_E \ln 2 + 41728 \ln^2 2 \right. \\
& + 151200 \ln G - 151200 \gamma_E \ln G - 240 \ln 2 \left( 231 + 640 \ln G \right) + 3175200 \zeta'(-5) \\
& \times \left. \left( \gamma_E + 2 \ln 2 - 12 \ln G \right) - 226800 \zeta'(-3) \left( -15 + 15\gamma_E + 16 \ln 2 \right) + 204120000 \zeta'(-3)^2 \right) \Bigg\} \Bigg\} (23)
\end{aligned}$$

where  $\hat{\Lambda} = \Lambda/2\pi T$ ,  $\hat{\mu} = \mu/2\pi T$ ,  $G \approx 1.2824$  is Glaisher's constant and  $\gamma_E \approx 0.5772$  is Euler-Mascheroni constant.

### B. Gauge boson free energy in a strongly magnetized medium

The general structure of gauge boson self-energy can be written from Ref. [76] as

$$\Pi^{\mu\nu} = \alpha B^{\mu\nu} + \beta R^{\mu\nu} + \gamma Q^{\mu\nu} + \delta N^{\mu\nu}, \quad (24)$$

where  $\alpha$ ,  $\beta$ ,  $\gamma$  and  $\delta$  are the form factors.  $B^{\mu\nu}$ ,  $R^{\mu\nu}$ ,  $Q^{\mu\nu}$  and  $N^{\mu\nu}$  are the basis tensors of gluon self-energy. The form factors are calculated in Ref. [76] for zero quark chemical potential. Here we extend the calculation for nonzero quark chemical potential. The effect of nonzero quark chemical potential is reflected only in the Debye mass because the quark loop gets modified. But in the presence of a strong magnetic field the Debye mass does not change due to dimensional reduction. The form factors can be calculated as

$$\alpha = B^{\mu\nu} \Pi_{\mu\nu} = \frac{m_D^2}{\bar{u}^2} [1 - \mathcal{T}_P(p_0, p)] - \sum_f \frac{(\delta m_{D,f}^2)_s}{\bar{u}^2} e^{-p_\perp^2/2q_f B} \frac{p_3^2}{p_0^2 - p_3^2}, \quad (25)$$

$$\beta = R^{\mu\nu} \Pi_{\mu\nu} = \frac{m_D^2}{2} \left[ \frac{p_0^2}{p^2} - \frac{P^2}{p^2} \mathcal{T}_P(p_0, p) \right], \quad (26)$$

$$\gamma = Q^{\mu\nu}\Pi_{\mu\nu} = \frac{m_D^2}{2} \left[ \frac{p_0^2}{p^2} - \frac{P^2}{p^2} \mathcal{T}_P(p_0, p) \right] + \sum_f \frac{(\delta m_{D,f}^2)_s}{\bar{u}^2} e^{-p_\perp^2/2q_f B} \frac{p_3^2}{p_0^2 - p_3^2}, \quad (27)$$

$$\delta = \frac{1}{2} N^{\mu\nu}\Pi_{\mu\nu} = \sum_f (\delta m_{D,f}^2)_s \frac{\sqrt{\bar{n}^2}}{\sqrt{\bar{u}^2}} e^{-p_\perp^2/2eB} \frac{p_0 p_3}{p_0^2 - p_3^2}, \quad (28)$$

where  $\bar{u}^2 = -p^2/P^2$ ,  $\bar{n}^2 = -p_\perp^2/p^2$  and

$$\mathcal{T}_P(p_0, p) = \frac{p_0}{2p} \ln \frac{p_0 + p}{p_0 - p}. \quad (29)$$

The thermal and magnetic correction of the Debye screening mass is given as

$$m_D^2 = \frac{g^2 N_c T^2}{3}, \quad (30)$$

$$\begin{aligned} (\delta m_{D,f}^2)_s &= \frac{g^2 |q_f B|}{2\pi T} \int_{-\infty}^{\infty} \frac{dk_3}{4\pi} \left[ n_F(k_3 + \mu) \left\{ 1 - n_F(k_3 + \mu) \right\} + n_F(k_3 - \mu) \left\{ 1 - n_F(k_3 - \mu) \right\} \right] \\ &= \frac{g^2 |q_f B|}{4\pi^2}, \end{aligned} \quad (31)$$

$$(m_D^s)^2 = m_D^2 + \sum_f (\delta m_{D,f}^2)_s = m_D^2 + (\delta m_D^2)_s. \quad (32)$$

The total gluon free-energy expanded up to  $\mathcal{O}[g^4]$  is given by

$$F_g \approx d_A \left[ \sum_{\substack{f \\ P}} \ln(-P^2) - \frac{\alpha + \beta + \gamma}{2P^2} - \frac{\alpha^2 + \beta^2 + \gamma^2 + 2\delta^2}{4P^4} \right] \quad (33)$$

where  $d_A = N_c^2 - 1$ .

The gluon free energy is calculated in details in Ref. [53]. Here we give the final expression.

The renormalized total gluon free energy containing both hard and soft contributions is given as

$$\begin{aligned} F_g^r &= \frac{d_A}{(4\pi)^2} \left[ -\frac{16\pi^4 T^4}{45} + \frac{2C_A g^2 \pi^2 T^4}{9} + \frac{1}{12} \left( \frac{C_A g^2 T^2}{3} \right)^2 \left( 8 - 3\gamma_E - \pi^2 + 4 \ln 2 - 3 \ln \frac{\hat{\Lambda}}{2} \right) \right. \\ &\quad + \frac{2N_f \pi^2 T^2}{9} \left( \frac{g^2}{4\pi^2} \right)^2 \sum_f q_f B \left( 36 \ln G - 4 + 3 \ln \hat{\Lambda} \right) + \left( N_f^2 + \sum_{f_1, f_2} \frac{q_{f_1} B}{q_{f_2} B} \right) \\ &\quad \times \frac{g^4 T^4}{32} \left( -\frac{12\zeta'(4)}{\pi^4} + \frac{2}{15} \left( \ln \frac{\hat{\Lambda}}{2} + \gamma_E + \ln 4\pi \right) - \frac{17}{75} \right) - \frac{1}{2} \left( \frac{g^2}{4\pi^2} \right)^2 \\ &\quad \times \sum_{f_1, f_2} q_{f_1} B q_{f_2} B \left( 4 - 4(\ln 2 - 1)(\ln \hat{\Lambda} + \gamma_E) - \frac{\pi^2}{3} + 2(\ln 2 - 2) \ln 2 \right) - \frac{C_A N_f g^4 T^4}{36} \\ &\quad \times \left( 3 - 24 \ln G - 2 \ln \frac{\hat{\Lambda}}{2} \right) - \sum_f \frac{C_A g^4 T^2 q_f B}{144\pi^2} \left( \pi^2 - 4 + 12 \ln \frac{\hat{\Lambda}}{2} - 2 \ln 2 \left( 6\gamma_E + 4 \right. \right. \\ &\quad \left. \left. + 3 \ln 2 - 6 \ln \frac{\hat{\Lambda}}{2} \right) + 12\gamma_E \right) \left. \right] - \frac{d_A (m_D^s)^3 T}{12\pi} \end{aligned} \quad (34)$$

where  $C_A = 3$  is the color factor which is associated with gluon emission from a gluon.

### C. QCD coupling constant

In the strong magnetic field region we use the QCD coupling constant obtained in Ref. [77] which depends on both momentum transfer and magnetic field

$$\alpha_s(\Lambda^2, |eB|) = \frac{\alpha_s(\Lambda^2)}{1 + b_1 \alpha_s(\Lambda^2) \ln \left( \frac{\Lambda^2}{\Lambda^2 + |eB|} \right)} \quad (35)$$

where the one-loop running coupling in the absence of magnetic field is given by

$$\alpha_s(\Lambda^2) = \frac{1}{b_1 \ln \left( \Lambda^2 / \Lambda_{\overline{MS}}^2 \right)}, \quad (36)$$

with  $b_1 = \frac{11N_c - 2N_f}{12\pi}$  and  $\Lambda_{\overline{MS}} = 176$  MeV [78] at  $\alpha_s(1.5\text{GeV}) = 0.326$  for  $N_f = 3$ . In Sec. IV we use the coupling constant defined in Eq. (36) which is independent of the magnetic field as the corresponding magnetic field is feeble.

### D. Longitudinal and transverse pressure and corresponding susceptibilities

Free energy density of the quark-gluon plasma in the presence of a strong magnetic field is given by

$$F = u - Ts - \mu n - eB \cdot M, \quad (37)$$

where  $u$  is total the energy density and magnetization per unit volume is given by

$$M = -\frac{\partial F}{\partial(eB)}. \quad (38)$$

The pressure becomes anisotropic [53, 79] due to the magnetization acquired by the system in presence of strong magnetic field which results in two different pressure along parallel and perpendicular to the magnetic field direction. The longitudinal pressure is given as

$$P_z = -F = -(F_q^r + F_g^r). \quad (39)$$

and transverse pressure is given as

$$P_\perp = -F - eB \cdot M. \quad (40)$$

In the left panel of Fig. 2 we show the variation of longitudinal and transverse pressure with the strength of the magnetic field at  $\mu = 0$ . It can be seen that the longitudinal pressure (pressure

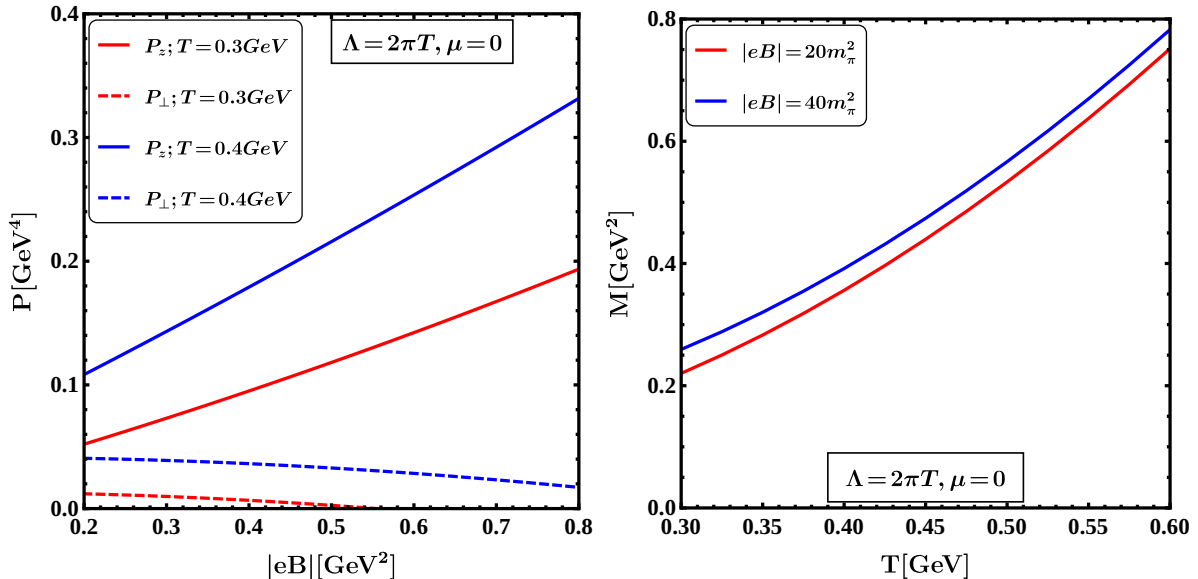


FIG. 2: Variation of the longitudinal and transverse pressure at  $\mu = 0$  with magnetic field is shown in left panel. Magnetization as a function of temperature at  $\mu = 0$  is shown in right panel for  $N_f = 3$ .

along the magnetic field direction) of magnetized quark-gluon plasma (QGP) increases with the magnetic field whereas the transverse pressure is opposite in nature. This indicates that the system may elongate along the longitudinal direction and compress along the transverse direction at a high magnetic field. In the right panel of Fig. 2 magnetization of the system is plotted with the temperature. The positive value of the magnetization implies paramagnetism of the strongly magnetized QCD medium which is also observed in recent lattice calculation [80]. It is noted that the pressure and magnetization plots of Fig. 2 shows qualitative matching with the lattice result of Ref. [80]. However, quantitatively the results are different due to the fact that one only gets correct perturbative coefficients of  $g^0$  and  $g^3$  in leading order of HTLpt. Thus one should go beyond one loop to get complete result up to  $\mathcal{O}(g^5)$ .

One gets two different second-order QNS, namely, along the longitudinal ( $\chi_z$ ) and transverse ( $\chi_\perp$ ) direction in the presence of a strong magnetic field. The longitudinal second-order QNS can be obtained as

$$\chi_z = \left. \frac{\partial^2 P_z}{\partial \mu^2} \right|_{\mu=0}, \quad (41)$$

whereas the transverse one can be obtained as

$$\chi_\perp = \left. \frac{\partial^2 P_\perp}{\partial \mu^2} \right|_{\mu=0}. \quad (42)$$

The longitudinal pressure of noninteracting quark-gluon gas in the presence of strong magnetic field is given as

$$P_{sf} = \sum_f N_c N_f q_f B \frac{T^2}{6} (1 + 12\hat{\mu}^2) + (N_c^2 - 1) \frac{\pi^2 T^4}{45}. \quad (43)$$

The second-order longitudinal QNS for the ideal quark gluon plasma is given as

$$\chi_{sf} = \sum_f N_c N_f \frac{q_f B}{\pi^2}. \quad (44)$$

The transverse pressure of ideal quark-gluon plasma is given as

$$P_{sf}^\perp = (N_c^2 - 1) \frac{\pi^2 T^4}{45}. \quad (45)$$

Thus, the second-order transverse QNS of the ideal quark-gluon plasma vanishes.

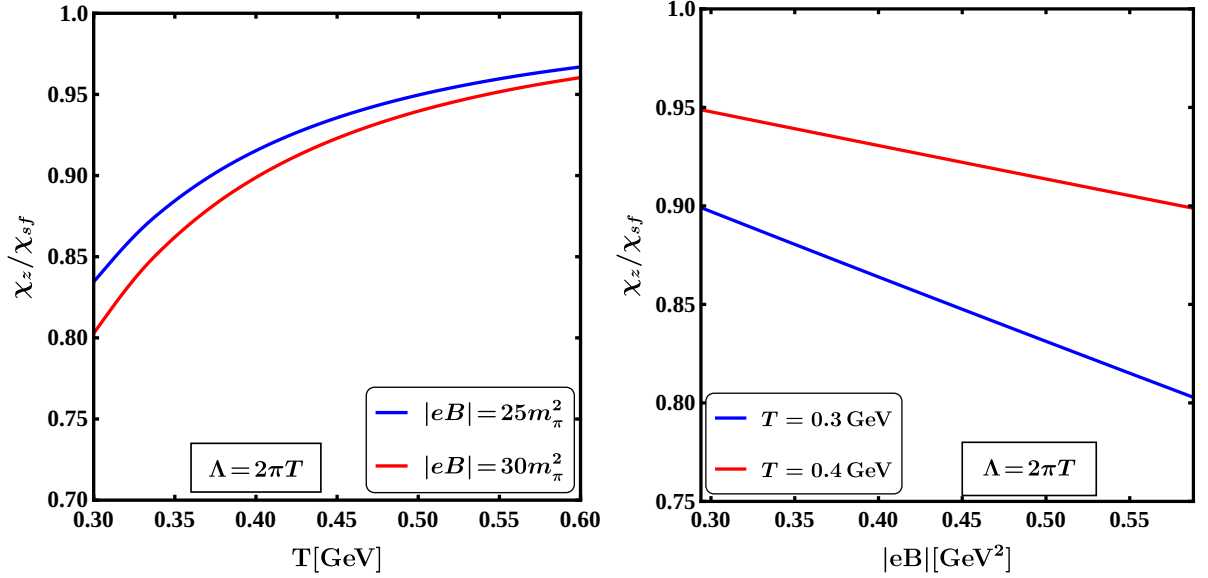


FIG. 3: Variation of the longitudinal part of the second-order QNS scaled with that of free field value in presence of strong magnetic field with temperature (left panel) and magnetic field (right panel) strength for  $N_f = 3$ .

In the left panel of Fig. 3 the variation of the longitudinal second-order QNS with temperature is displayed for two values of magnetic field strength and the central value of renormalization scale  $\Lambda = 2\pi T$ . For a given magnetic field strength the longitudinal second-order QNS is found to increase with temperature and approaches the free field value at high temperature. On the other

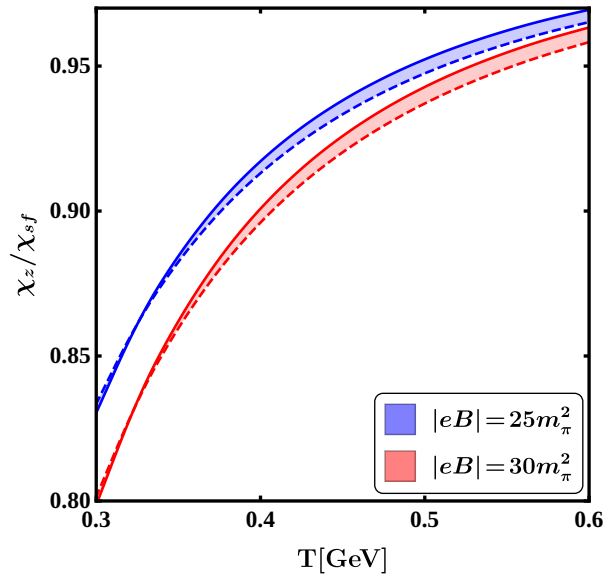


FIG. 4: Sensitivity of the longitudinal part of the second-order QNS scaled with that of free field value in presence of strong magnetic field on the renormalization scale for  $N_f = 3$ . The dashed and the continuous curves represent  $\Lambda = \pi T$  and  $\Lambda = 4\pi T$  respectively.

hand for a given temperature the longitudinal second-order QNS decreases with increase of the magnetic field strength as shown in the right panel of Fig. 3 for two different temperatures and the central value of renormalization scale  $\Lambda = 2\pi T$ .

The QGP pressure as well as the second order QNS is dependent on the renormalization scale  $\Lambda$ . Fig. 4 shows the sensitivity of the results on the choice of renormalization scale. Here we have varied it around the central value by a factor of two, i.e., from  $\pi T$  to  $4\pi T$ .

In the left panel of Fig. 5 the variation of transverse second-order QNS with temperature is displayed for two values of magnetic field strength and the central value of renormalization scale  $\Lambda = 2\pi T$ . It is found that the transverse second-order QNS decreases with temperature. This is an indication that the system may shrink in the transverse direction. For a given temperature the transverse second-order QNS is found to increase with the increase of the magnetic field strength as shown in the right panel of Fig. 5 for two different temperatures and the central value of renormalization scale  $\Lambda = 2\pi T$ . This behaviour is in contrary to that of the longitudinal one. In Fig. 6 the sensitivity of the transverse second order QNS on the renormalization scale is displayed by varying a factor of two around the central value  $\Lambda = 2\pi T$ .

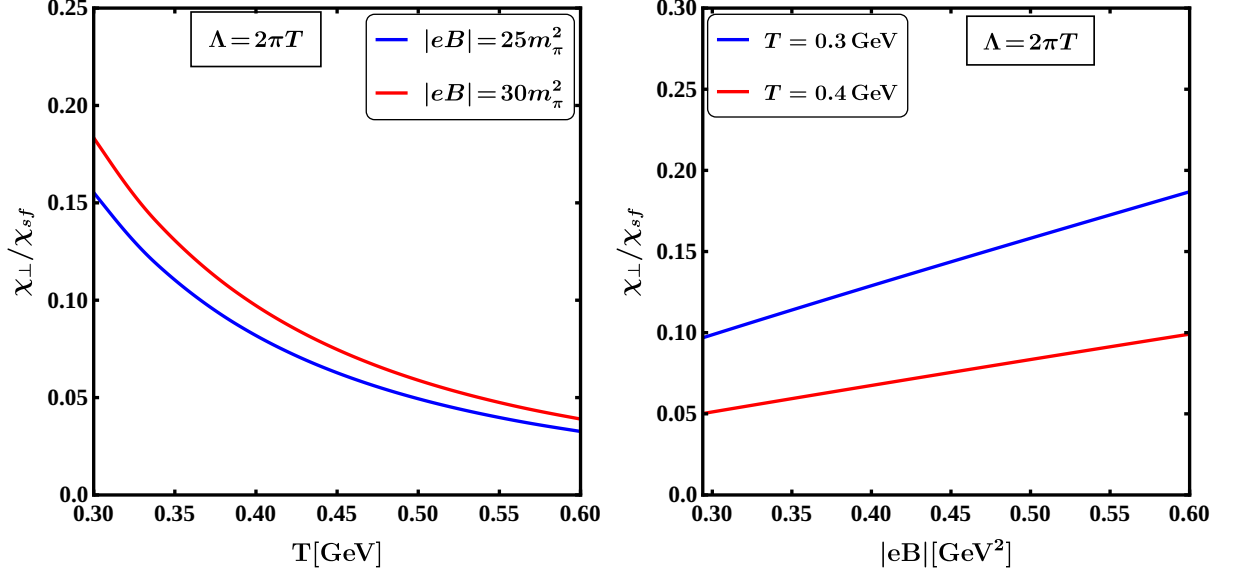


FIG. 5: Variation of the transverse part of the second-order QNS scaled with that of free field value in presence of strong magnetic field with temperature (left panel) and magnetic field (right panel) strength for  $N_f = 3$ .

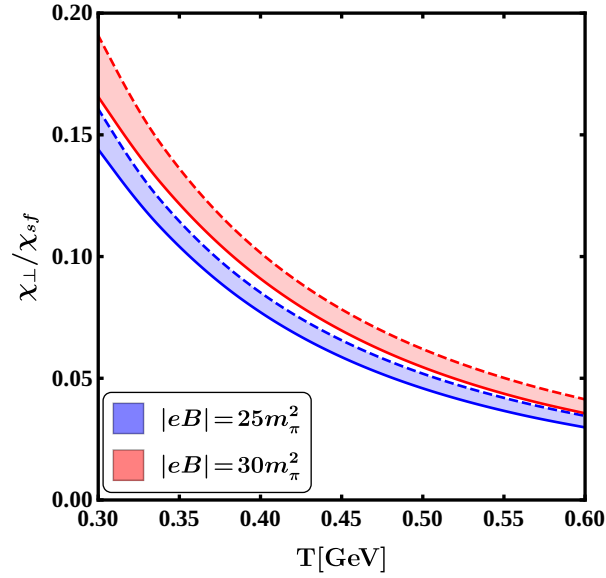


FIG. 6: Sensitivity of the transverse QNS scaled with that of free field value in presence of strong magnetic field on the renormalization scale for  $N_f = 3$ . The dashed and the continuous curves represent  $\Lambda = \pi T$  and  $\Lambda = 4\pi T$  respectively.

The second-order quark number susceptibility represents the fluctuation of net quark number over the average value. As the system becomes anisotropic in presence of strong magnetic field, we

get two different pressure along the longitudinal and transverse direction to the magnetic field. It has been shown [53] in Fig. 2 that the magnitude of the longitudinal pressure is greater than the transverse pressure. Thus the system expands more along the longitudinal direction. Similarly, one gets two different quark number susceptibility along the longitudinal and transverse direction. We can see from Eq. (44) that the longitudinal QNS of ideal quark gluon plasma in presence of strong magnetic field depends only on the strength of the magnetic field. However, the longitudinal QNS of the interacting quark gluon plasma depends both on temperature and magnetic field. This increases with temperature and matches with the ideal (non-interacting) QNS at very high temperatures which can be seen from Fig. 7. However, transverse QNS behaves very differently from the longitudinal one due to the presence of magnetization which can be understood as follows. Transverse QNS of ideal quark gluon plasma is zero due to the fact that only gluon contributes to the ideal transverse pressure. Momentum of the quarks become restricted to the direction of magnetic field due to the dimensional reduction in presence of strong magnetic field. Hence the transverse pressure only consists of gluon pressure. Now, in presence of interaction one gets a non-zero transverse QNS because the transverse pressure gets contribution from internal quark loop. The transverse QNS gradually vanishes at high temperature (free limit) as can be seen from Fig. 7.

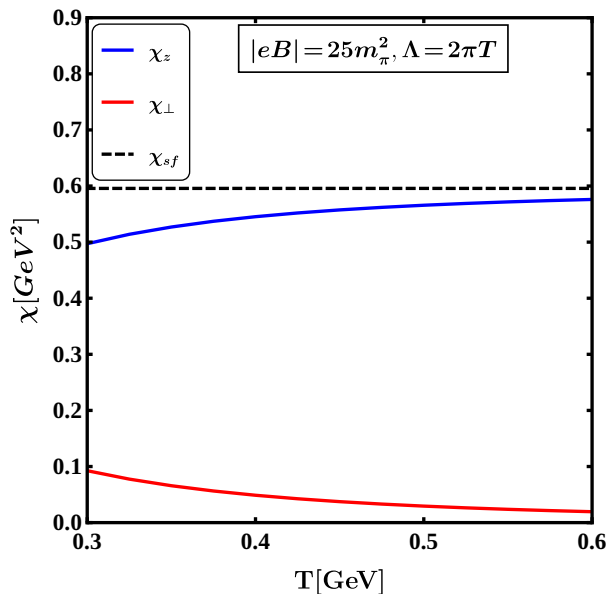


FIG. 7: Variation of longitudinal and transverse QNS with temperature in presence of strong magnetic field.

#### IV. WEAK MAGNETIC FIELD

In this section we consider magnetic field strength to be the lowest among all the scales  $T$ ,  $m_{th}$  as  $\sqrt{|q_f B|} < m_{th} \sim gT < T$ . The HTL one-loop free-energy for the deconfined QCD matter has been calculated upto  $\mathcal{O}[g^4]$  in Ref. [54]. The total renormalized free-energy in presence of weak magnetic field is sum of renormalized quark and gluon free-energy and can be written [54] as

$$F = F_q^r + F_g^r, \quad (46)$$

where the renormalized quark free-energy is

$$\begin{aligned} F_q^r = N_c N_f \left[ -\frac{7\pi^2 T^4}{180} \left( 1 + \frac{120\hat{\mu}^2}{7} + \frac{240\hat{\mu}^4}{7} \right) + \frac{g^2 C_F T^4}{48} (1 + 4\hat{\mu}^2) (1 + 12\hat{\mu}^2) \right. \\ \left. + \frac{g^4 C_F^2 T^4}{768\pi^2} (1 + 4\hat{\mu}^2)^2 (\pi^2 - 6) + \frac{g^4 C_F^2}{27N_f} M_B^4 \left( 12 \ln \frac{\hat{\Lambda}}{2} - 6\aleph(z) + \frac{36\zeta(3)}{\pi^2} \right. \right. \\ \left. \left. - 2 - \frac{72}{\pi^2} \right) \right]. \end{aligned} \quad (47)$$

$M_{B,f}$  is the thermomagnetic mass for quark flavor  $f$  in presence of weak magnetic field and  $M_B$  represents flavor summed thermomagnetic quark mass as

$$M_B^2 = \sum_f M_{B,f}^2 = \sum_f \frac{q_f B}{16\pi^2} \left[ -\frac{1}{4}\aleph(z) - \frac{\pi T}{2m_f} - \frac{\gamma_E}{2} \right]. \quad (48)$$

$\aleph(z)$  in Eq. (47) is abbreviated as

$$\aleph(z) \equiv \Psi(z) + \Psi(z^*), \quad (49)$$

with  $\Psi(z)$  is the digamma function

$$\Psi(z) \equiv \frac{\Gamma'(z)}{\Gamma(z)}, \quad (50)$$

and  $z = 1/2 - i\hat{\mu}$ . At small chemical potential,  $\aleph(z)$  can be expanded as

$$\aleph(z) = -2\gamma_E - 4 \ln 2 + 14\zeta(3)\hat{\mu}^2 - 62\zeta(5)\hat{\mu}^4 + 254\zeta(7)\hat{\mu}^6 + \mathcal{O}(\hat{\mu}^8). \quad (51)$$

In addition to the renormalized quark free-energy in Eq. (47), the renormalized gluon free-energy is given as

$$\begin{aligned} \frac{F_g^r}{d_A} = -\frac{\pi^2 T^4}{45} \left[ 1 - \frac{15}{2}\hat{m}_D^2 + 30(\hat{m}_D^w)^3 + \frac{45}{8}\hat{m}_D^4 \left( 2 \ln \frac{\hat{\Lambda}}{2} - 7 + 2\gamma_E + \frac{2\pi^2}{3} \right) \right] \\ - \pi^2 T^4 \hat{m}_D^2 \delta \hat{m}_D^2 \left( \gamma_E + \ln \hat{\Lambda} \right) + \sum_f \frac{g^2 (q_f B)^2 T^2}{(12\pi)^2 m_f^2} \left[ 4.97 + 2 \ln \frac{\hat{\Lambda}}{2} \right] \end{aligned}$$

$$\begin{aligned}
& + 3\hat{m}_D^2 \left\{ 2(1 - \ln 2) \ln^2 \frac{\hat{\Lambda}}{2} + 2 \left( \frac{7}{2} - \frac{\pi^2}{6} - \ln^2(2) - 2\gamma_E(\ln 2 - 1) \right) \ln \frac{\hat{\Lambda}}{2} + 4.73 \right\} \\
& - \sum_f \frac{g^2(q_f B)^2}{(12\pi)^2} \frac{\pi T}{32m_f} \left[ \left\{ \frac{3}{4} \ln^2 \frac{\hat{\Lambda}}{2} + 2 \ln \frac{\hat{\Lambda}}{2} \left( \frac{21}{8} + \frac{3}{4} \frac{\zeta'(-1)}{\zeta(-1)} + \frac{27}{4} \ln 2 \right) + 43.566 \right. \right. \\
& + \frac{3}{4} \hat{m}_D^2 \left[ 2 \ln^2 \frac{\hat{\Lambda}}{2} \left( 5\pi^2 - \frac{609}{10} + \frac{114 \ln 2}{5} \right) + 2 \ln \frac{\hat{\Lambda}}{2} \left( 30\zeta(3) - \frac{5779}{75} + \frac{121}{6} \pi^2 + \frac{114}{5} \ln^2(2) \right. \right. \\
& + \left. \left. \frac{468}{25} \ln 2 + \gamma_E \left( 10\pi^2 - \frac{609}{5} + \frac{228}{5} \ln 2 \right) \right) + 106.477 \right] \left. \right\} + \frac{8}{3\pi} \left\{ (3 \ln 2 - 4) \ln \frac{\hat{\Lambda}}{2} - 3.92 \right. \\
& + 3\hat{m}_D^2 \left[ \frac{1}{20} \ln^2 \frac{\hat{\Lambda}}{2} \left( 11 + 5\pi^2 - 92 \ln 2 \right) + 2 \ln \frac{\hat{\Lambda}}{2} \left( \frac{3}{4} \zeta(3) + \frac{1557}{200} - \frac{\pi^2}{3} - \frac{23}{10} \ln^2(2) \right. \right. \\
& \left. \left. - \frac{168}{25} \ln 2 + \gamma_E \left( \frac{11}{20} + \frac{\pi^2}{4} - \frac{23}{5} \ln 2 \right) \right) - 1.86 \right] \left. \right\}, \tag{52}
\end{aligned}$$

where  $\hat{m}_D^w = m_D^w/2\pi T$ ,  $\hat{m}_D = m_D/2\pi T$ ,  $\delta\hat{m}_D = \delta m_D/2\pi T$  and  $m_D^w$  represents the Debye mass in weak magnetic field approximation and is obtained as

$$\begin{aligned}
(m_D^w)^2 & \simeq \frac{g^2 T^2}{3} \left[ \left( N_c + \frac{N_f}{2} \right) + 6N_f \hat{\mu}^2 \right] \\
& + \sum_f \frac{g^2 (q_f B)^2}{12\pi^2 T^2} \sum_{l=1}^{\infty} (-1)^{l+1} l^2 \cosh(2l\pi\hat{\mu}) K_0 \left( \frac{m_f l}{T} \right) + \mathcal{O}[(q_f B)^4] \\
& = m_D^2 + \delta m_D^2. \tag{53}
\end{aligned}$$

Considering the expression of free energy vis-a-vis pressure we calculate the second-order QNS in weak field limit by using Eq. (4). The second-order QNS of free quarks and gluons in thermal medium is given as

$$\chi_f = \frac{1}{3} N_c N_f T^2. \tag{54}$$

The left panel of Fig. 8 shows the variation of the scaled second-order QNS with the temperature at different values of the magnetic field strength and the central value of renormalization scale  $\Lambda = 2\pi T$ . The weak field effect appears as a correction to the thermal medium, the weak field second-order QNS is not very much different than that of thermal medium. It is found to increase with temperature and approaches the free field value at high enough temperature. The magnetic field effect on the second-order QNS is visible at low temperature. The value of second-order QNS slowly decreases as one increases the magnetic field strength as shown in the right panel of Fig. 8. In Fig. 9 the sensitivity of the second order weak field QNS on the renormalization scale is displayed by varying a factor of two around the central value  $\Lambda = 2\pi T$ .

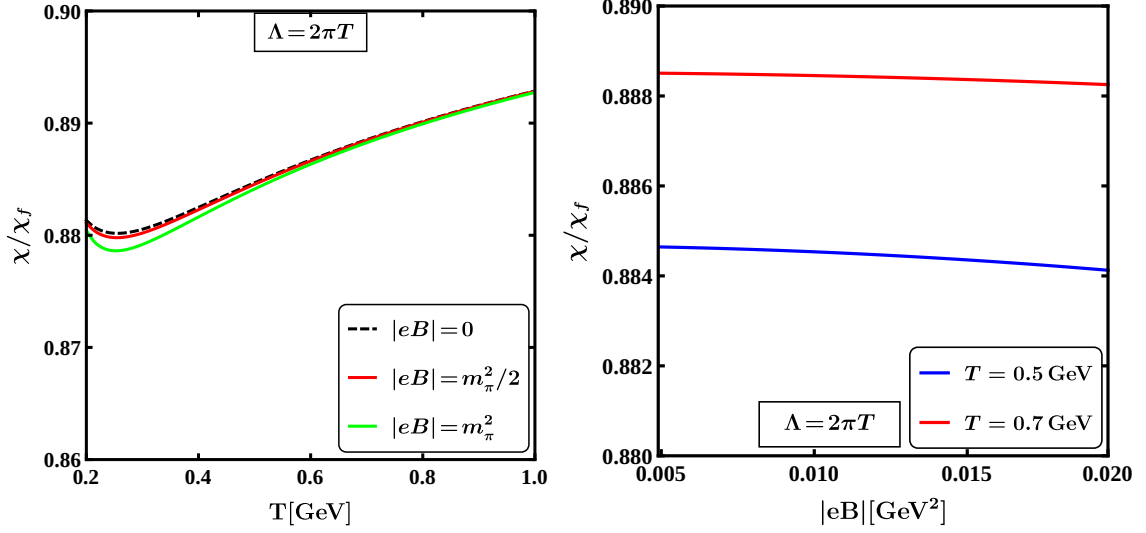


FIG. 8: Variation of second-order QNS scaled with thermal free field value with temperature (left panel) and magnetic field strength (right panel) for  $m_f = 5$  MeV and  $N_f = 3$ .

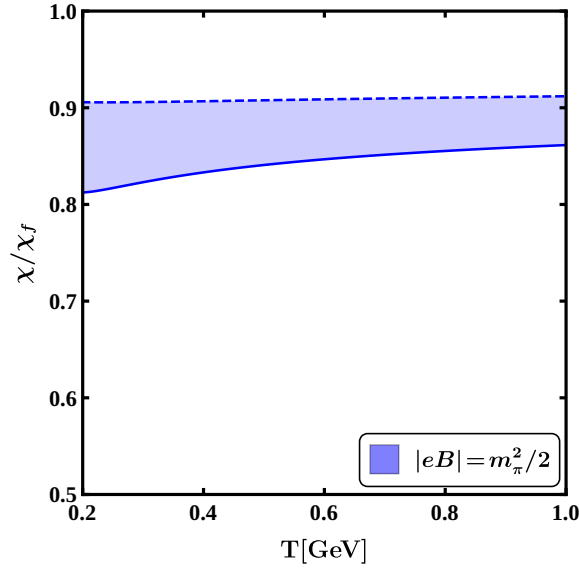


FIG. 9: Sensitivity of the second-order QNS scaled with that of free field value in presence of weak magnetic field on the renormalization scale for  $N_f = 3$ . The dashed and the continuous curves represent  $\Lambda = \pi T$  and  $\Lambda = 4\pi T$  respectively.

## V. CONCLUSION

We consider a hot and dense deconfined QCD matter in the presence of the background strong and weak magnetic field within HTL approximation. The quarks are directly affected by magnetic

field whereas gluons are affected via quark loop in the gluon self-energy. In the strong field approximation we assume quarks are in lowest Landau level. We compute the one-loop HTL pressure in the presence of finite temperature and chemical potential in the lowest Landau level within the strong field approximation. Various divergent terms are eliminated by choosing appropriate counterterms in the  $\overline{\text{MS}}$  renormalization scheme. The presence of magnetization causes the system to be anisotropic, and one obtains two different pressures in directions parallel and perpendicular to the magnetic field. Both the longitudinal and transverse pressures are computed analytically by calculating the magnetization of the system. We then compute both the longitudinal and transverse second-order QNS in the strong field approximation. For a given magnetic field strength, the longitudinal second-order QNS increases with temperature and approaches the non-interacting value at high enough temperature. For a given temperature the longitudinal second-order QNS is found to decrease with increase of magnetic field strength. In contrast the transverse second-order QNS is found to decrease with temperature and increase with the increase of magnetic field. Further, in weak field approximation we consider one-loop HTL pressure of hot and dense QCD matter of Ref. [54] and compute the second-order QNS. The thermomagnetic correction is found to be marginal and slowly varies with magnetic field. Our calculation can be compared with future lattice QCD calculation.

## VI. ACKNOWLEDGMENTS

BK and MGM were funded by Department of Atomic Energy (DAE), India via the project TPAES. NH was funded by DAE, India. BK acknowledges useful discussions with Arghya Mukherjee and Aritra Bandyopadhyay.

### Appendix A: Calculation of the quark self-energy form factors

#### 1. Calculation of the form factors $a$ and $d$

We denote the momentum four-vectors as  $K^\mu = (k_0, k_1, k_2, k_3)$  and we decompose the four-vector  $K^\mu$  into its parallel and perpendicular components as  $K_\parallel^\mu = (K \cdot u)u^\mu - (K \cdot n)n^\mu = (k_0, 0, 0, k_3)$  and  $K_\perp^\mu = K^\mu - K_\parallel^\mu = (0, k_1, k_2, 0)$ . Thus the scalar product becomes  $K_\perp^\mu \cdot (K_\perp)_\mu = K_\perp^2 = -k_\perp^2 = -k_1^2 - k_2^2$ .

Now, we can calculate the form factor  $a$  from Eq. (6) as

$$a = \frac{1}{4} \text{Tr}[\Sigma\psi] = -2g^2 C_F \sum_{\{k_0\}} e^{-\frac{k_\perp^2}{q_f B}} \left[ \frac{k_0}{K_\parallel^2 (K-P)_\parallel^2} + (k-p)_\perp^2 \frac{k_0}{K_\parallel^2 (K-P)_\parallel^4} \right] \quad (\text{A1})$$

where  $g$  is the QCD coupling constant,  $C_F = 4/3$  is the Casimir color-factor associated with gluon emission from a quark and  $q_f$  is the charge of the fermion of flavor  $f$ . The sum-integral is given as

$$\sum_{\{k_0\}} \equiv T \sum_{k_0=(2n+1)\pi T i + \mu} \int \frac{d^3 k}{(2\pi)^3}. \quad (\text{A2})$$

So, Eq. (A1) becomes

$$\begin{aligned} a &= -2g^2 C_F \int \frac{d^3 k}{(2\pi)^3} e^{-\frac{k_\perp^2}{q_f B}} [T_2 + (k-p)_\perp^2 T_4] \\ &= -2g^2 C_F \int_{-\infty}^{\infty} \frac{dk_3}{2\pi} \left[ \frac{q_f B}{4\pi} T_2 + \frac{q_f B}{4\pi} (p_\perp^2 + q_f B) T_4 \right] \\ &= -\frac{g^2 C_F (q_f B)}{4\pi^2} \int_{-\infty}^{\infty} dk_3 [T_2 + (p_\perp^2 + q_f B) T_4], \end{aligned} \quad (\text{A3})$$

where

$$\begin{aligned} T_2 &= \sum_{\{k_0\}} \frac{k_0}{K_\parallel^2 (K-P)_\parallel^2}, \\ T_4 &= \sum_{\{k_0\}} \frac{k_0}{K_\parallel^2 (K-P)_\parallel^4} = -\frac{1}{2k_3} \frac{\partial T_2}{\partial p_3}. \end{aligned} \quad (\text{A4})$$

Here we also note that in LLL,  $p_\perp = 0$ . Now we perform the Matsubara sum [81] and use HTL approximations (loop momentum  $\sim T$ , external momentum  $\sim gT$ ).

$$\begin{aligned} T_2 &= \sum_{\{k_0\}} \frac{k_0}{K_\parallel^2 (K-P)_\parallel^2}, \\ &= -\frac{1}{4k_3} \left[ \frac{n_B(k_3) + n_F(k_3 - \mu)}{p_0 + p_3} + \frac{n_B(k_3) + n_F(k_3 + \mu)}{p_0 - p_3} \right] \end{aligned} \quad (\text{A5})$$

We use the following equations to perform the sum-integrals.

$$\begin{aligned} \int_{-\infty}^{\infty} \frac{dk_3}{k_3} n_F(k_3 \pm \mu) &= 2 \int_0^{\infty} \frac{dk_3}{k_3} n_F(k_3 \pm \mu), \\ \int_{-\infty}^{\infty} \frac{dk_3}{k_3^2} n_F(k_3 \pm \mu) &= 2 \int_0^{\infty} \frac{dk_3}{k_3^2} n_F(k_3 \pm \mu). \end{aligned} \quad (\text{A6})$$

Hence,

$$\begin{aligned} &\int_{-\infty}^{\infty} dk_3 T_2 \\ &= -\int_0^{\infty} \frac{dk_3}{4k_3} \left[ \frac{2n_B(k_3) + 2n_F(k_3 - \mu)}{p_0 + p_3} + \frac{2n_B(k_3) + 2n_F(k_3 + \mu)}{p_0 - p_3} \right] \end{aligned}$$

$$\begin{aligned}
&= - \int_0^\infty \frac{dk_3}{4k_3} \left( 2n_B(k_3) \frac{2p_0}{p_0^2 - p_3^2} + \frac{2n_F(k_3 + \mu)}{p_0 - p_3} + \frac{2n_F(k_3 - \mu)}{p_0 + p_3} \right) \\
&= \frac{p_0}{p_0^2 - p_3^2} \left[ \ln 2 - \frac{\mu^2}{T^2} \frac{7\zeta(3)}{8\pi^2} + \frac{\mu^4}{T^4} \frac{31\zeta(5)}{32\pi^4} \right] + \frac{p_3}{p_0^2 - p_3^2} \left[ \frac{\mu}{4T} \left( -1 - \gamma_E - \frac{4}{3} \ln 2 \right. \right. \\
&\quad \left. \left. + 12 \ln G \right) + \frac{\mu^3}{48T^3} \left( \gamma_E + \frac{16}{15} \ln 2 - 120\zeta'(-3) \right) + \mathcal{O}[(\mu/T)^5] \right], \tag{A7}
\end{aligned}$$

where  $G \approx 1.2824$  is Glaisher's constant and  $\zeta'(z) = \frac{d\zeta(z)}{dz} = -\sum_{n=2}^\infty \frac{\ln n}{n^z}$ .

$$\begin{aligned}
&\int_{-\infty}^\infty dk_3 q_f B T_4 \\
&= -\frac{q_f B}{2} \frac{\partial}{\partial p_3} \int_{-\infty}^\infty \frac{dk_3}{k_3} T_2 \\
&= \frac{q_f B}{2} \frac{\partial}{\partial p_3} \int_{-\infty}^\infty \frac{dk_3}{4k_3^2} \left( \frac{n_B(k_3) + n_F(k_3 - \mu)}{p_0 + p_3} + \frac{n_B(k_3) + n_F(k_3 + \mu)}{p_0 - p_3} \right) \\
&= \frac{q_f B}{2} \frac{\partial}{\partial p_3} \int_0^\infty \frac{dk_3}{4k_3^2} \left( 2n_B(k_3) \frac{2p_0}{p_0^2 - p_3^2} + \frac{2n_F(k_3 + \mu)}{p_0 - p_3} + \frac{2n_F(k_3 - \mu)}{p_0 + p_3} \right) \\
&= \frac{q_f B}{T} \left[ \frac{p_0 p_3}{(p_0^2 - p_3^2)^2} \left\{ \frac{1}{6} (\gamma_E + 2 \ln 2 - 12 \ln G) + \frac{\mu^2}{16T^2} \left( 1 - \gamma_E - \frac{16}{15} \ln 2 \right. \right. \right. \\
&\quad \left. \left. + 120\zeta'(-3) \right) + \frac{\mu^4}{96T^4} \left( -1 + \gamma_E + \frac{64}{63} \ln 2 + 252\zeta'(-5) \right) \right\} + \frac{p_0^2 + p_3^2}{(p_0^2 - p_3^2)^2} \\
&\quad \times \left\{ \frac{\mu}{T} \frac{7\zeta(3)}{8\pi^2} - \frac{\mu^3}{T^3} \frac{31\zeta(5)}{16\pi^4} \right\} + \mathcal{O}[(\mu/T)^5] \right]. \tag{A8}
\end{aligned}$$

So the form factor  $a = -d$  upto  $\mathcal{O}[(\mu/T)^4]$  can be written in compact form as

$$a = -d = c_1 \left[ \frac{p_0}{P_{||}^2} c_2 + \frac{p_3}{P_{||}^2} c_3 + \frac{p_0 p_3}{P_{||}^4} c_4 + \left( \frac{1}{P_{||}^2} + \frac{2p_3^2}{P_{||}^4} \right) c_5 \right] \tag{A9}$$

where

$$\begin{aligned}
c_1 &= -\frac{g^2 C_F (q_f B)}{4\pi^2}, \\
c_2 &= \left[ \ln 2 - \frac{\mu^2}{T^2} \frac{7\zeta(3)}{8\pi^2} + \frac{\mu^4}{T^4} \frac{31\zeta(5)}{32\pi^4} \right], \\
c_3 &= \left[ \frac{\mu}{4T} \left( -1 - \gamma_E - \frac{4}{3} \ln 2 + 12 \ln G \right) + \frac{\mu^3}{48T^3} \left( \gamma_E + \frac{16}{15} \ln 2 - 120\zeta'(-3) \right) \right], \\
c_4 &= \frac{q_f B}{T} \left[ \frac{1}{6} (\gamma_E + 2 \ln 2 - 12 \ln G) + \frac{\mu^2}{16T^2} \left( 1 - \gamma_E - \frac{16}{15} \ln 2 + 120\zeta'(-3) \right) \right. \\
&\quad \left. + \frac{\mu^4}{96T^4} \left( -1 + \gamma_E + \frac{64}{63} \ln 2 + 252\zeta'(-5) \right) \right], \\
c_5 &= \frac{q_f B}{T} \left[ \frac{\mu}{T} \frac{7\zeta(3)}{8\pi^2} - \frac{\mu^3}{T^3} \frac{31\zeta(5)}{16\pi^4} \right]. \tag{A10}
\end{aligned}$$

## 2. Calculation of quark form factor $b$ and $c$

Similarly one can calculate  $b$  from Eq. (7) as

$$\begin{aligned}
b &= -\frac{1}{4} \text{Tr}[\Sigma \not{n}] = 2g^2 C_F \sum_{\{k_0\}} e^{-\frac{k_\perp^2}{q_f B}} \left[ \frac{k_3}{K_\parallel^2 (K-P)_\parallel^2} + (k-p)_\perp^2 \frac{k_3}{K_\parallel^2 (K-P)_\parallel^4} \right] \\
&= 2g^2 C_F \int \frac{d^3 k}{(2\pi)^3} e^{-\frac{k_\perp^2}{q_f B}} k_3 [T_1 + (k-p)_\perp^2 T_3] \\
&= 2g^2 C_F \int_{-\infty}^{\infty} \frac{dk_3}{2\pi} k_3 \left[ \frac{q_f B}{4\pi} T_1 + \frac{q_f B}{4\pi} (q_f B) T_3 \right] \\
&= \frac{g^2 C_F (q_f B)}{4\pi^2} \int_{-\infty}^{\infty} dk_3 k_3 [T_1 + q_f B T_3], \tag{A11}
\end{aligned}$$

where

$$T_1 = \sum_{\{k_0\}} \frac{1}{K_\parallel^2 (K-P)_\parallel^2}, \tag{A12}$$

$$T_3 = \sum_{\{k_0\}} \frac{1}{K_\parallel^2 (K-P)_\parallel^4} = -\frac{1}{2k_3} \frac{\partial T_1}{\partial p_3}. \tag{A13}$$

After doing the Matsubara sum, Eq. (A12) becomes

$$T_1 = \frac{1}{4k_3^2} \left[ \frac{n_B(k_3) + n_F(k_3 - \mu)}{p_0 + p_3} - \frac{n_B(k_3) + n_F(k_3 + \mu)}{p_0 - p_3} \right]. \tag{A14}$$

Hence,

$$\begin{aligned}
&\int_{-\infty}^{\infty} dk_3 k_3 T_1 \\
&= \int_0^{\infty} \frac{dk_3}{4k_3} \left[ \frac{2n_B(k_3) + 2n_F(k_3 - \mu)}{p_0 + p_3} - \frac{2n_B(k_3) + 2n_F(k_3 + \mu)}{p_0 - p_3} \right] \\
&= - \int_0^{\infty} \frac{dk_3}{4k_3} \left( 2n_B(k_3) \frac{2p_3}{p_0^2 - p_3^2} + \frac{2n_F(k_3 + \mu)}{p_0 - p_3} - \frac{2n_F(k_3 - \mu)}{p_0 + p_3} \right) \\
&= \frac{p_3}{p_0^2 - p_3^2} \left[ \ln 2 - \frac{\mu^2}{T^2} \frac{7\zeta(3)}{8\pi^2} + \frac{\mu^4}{T^4} \frac{31\zeta(5)}{32\pi^4} \right] + \frac{p_0}{p_0^2 - p_3^2} \left[ \frac{\mu}{4T} \left( -1 - \gamma_E - \frac{4}{3} \ln 2 \right. \right. \\
&\quad \left. \left. + 12 \ln G \right) + \frac{\mu^3}{48T^3} \left( \gamma_E + \frac{16}{15} \ln 2 - 120\zeta'(-3) \right) + \mathcal{O}[(\mu/T)^5] \right] \tag{A15}
\end{aligned}$$

and

$$\begin{aligned}
&\int_{-\infty}^{\infty} dk_3 k_3 q_f B T_3 \\
&= -\frac{q_f B}{2} \frac{\partial}{\partial p_3} \int_{-\infty}^{\infty} dk_3 T_1
\end{aligned}$$

$$\begin{aligned}
&= -\frac{q_f B}{2} \frac{\partial}{\partial p_3} \int_{-\infty}^{\infty} \frac{dk_3}{4k_3^2} \left[ \frac{n_B(k_3) + n_F(k_3 - \mu)}{p_0 + p_3} - \frac{n_B(k_3) + n_F(k_3 + \mu)}{p_0 - p_3} \right] \\
&= \frac{q_f B}{2} \frac{\partial}{\partial p_3} \int_0^{\infty} \frac{dk_3}{4k_3^2} \left[ \frac{2n_B(k_3) + 2n_F(k_3 - \mu)}{p_0 + p_3} - \frac{2n_B(k_3) + 2n_F(k_3 + \mu)}{p_0 - p_3} \right] \\
&= -\frac{q_f B}{2} \frac{\partial}{\partial p_3} \int_0^{\infty} \frac{dk_3}{4k_3^2} \left[ 2n_B(k_3) \frac{2p_3}{p_0^2 - p_3^2} + \frac{2n_F(k_3 + \mu)}{p_0 - p_3} - \frac{2n_F(k_3 - \mu)}{p_0 + p_3} \right] \\
&= -\frac{q_f B}{T} \left[ \frac{p_0^2 + p_3^2}{(p_0^2 - p_3^2)^2} \left\{ \frac{1}{6} (\gamma_E + 2 \ln 2 - 12 \ln G) + \frac{\mu^2}{16T^2} \left( 1 - \gamma_E - \frac{16}{15} \ln 2 \right. \right. \right. \\
&\quad \left. \left. \left. + 120\zeta'(-3) \right) + \frac{\mu^4}{96T^4} \left( -1 + \gamma_E + \frac{64}{63} \ln 2 + 252\zeta'(-5) \right) \right\} + \frac{4p_0 p_3}{(p_0^2 - p_3^2)^2} \right. \\
&\quad \left. \times \left\{ \frac{\mu}{T} \frac{7\zeta(3)}{8\pi^2} - \frac{\mu^3}{T^3} \frac{31\zeta(5)}{16\pi^4} \right\} + \mathcal{O}[(\mu/T)^5] \right]. \tag{A16}
\end{aligned}$$

The form factor  $b = -c$  is obtained upto  $\mathcal{O}[(\mu/T)^4]$  as

$$b = -c = -c_1 \left[ \frac{p_3}{P_{||}^2} c_2 + \frac{p_0}{P_{||}^2} c_3 - \left( \frac{1}{P_{||}^2} + \frac{2p_3^2}{P_{||}^4} \right) c_4 - \frac{4p_0 p_3}{P_{||}^4} c_5 \right]. \quad (\text{A17})$$

## Appendix B: One-loop sum-integrals for quark free-energy

Eq. (19) can be rewritten as

$$F'_q = -4d_F \sum_f \frac{q_f B}{(2\pi)^2} \oint_{\{p_0\}} dp_3 \left[ \frac{ap_0}{P_{||}^2} + \frac{bp_3}{P_{||}^2} - \frac{a^2}{P_{||}^2} - \frac{b^2}{P_{||}^2} - \frac{2a^2 p_3^2}{P_{||}^4} - \frac{2b^2 p_3^2}{P_{||}^4} - \frac{4abp_0 p_3}{P_{||}^4} \right] \quad (\text{B1})$$

The various sum-integrals in Eq. B1 can be written using Eq. (A9) and Eq. (A17) as

$$\oint_{\{p_0\}} \frac{ap_0}{P_{||}^2} = c_1 \oint_{\{p_0\}} \left[ c_2 \left( \frac{1}{P_{||}^2} + \frac{p_3^2}{P_{||}^4} \right) + \frac{p_0 p_3}{P_{||}^4} c_3 + \left( \frac{p_3}{P_{||}^4} + \frac{p_3^3}{P_{||}^6} \right) c_4 + c_5 \left( \frac{p_0}{P_{||}^4} + \frac{2p_0 p_3^2}{P_{||}^6} \right) \right], \quad (\text{B2})$$

$$\sum_{\{p_0\}} \frac{bp_3}{P_{||}^2} = -c_1 \sum_{\{p_0\}} \left[ \frac{p_3^2}{P_{||}^4} c_2 + \frac{p_0 p_3}{P_{||}^4} c_3 - \left( \frac{p_3}{P_{||}^4} + \frac{2p_3^3}{P_{||}^6} \right) c_4 - \frac{4p_0 p_3^2}{P_{||}^6} c_5 \right], \quad (\text{B3})$$

$$\begin{aligned} \not\!\!\!\sum_{\{p_0\}} \frac{a^2}{P_\parallel^2} = & c_1^2 \not\!\!\!\sum_{\{p_0\}} \left[ \frac{p_0^2}{P_\parallel^6} c_2^2 + \frac{p_3^2}{P_\parallel^6} c_3^2 + \frac{p_0^2 p_3^2}{P_\parallel^{10}} c_4^2 + \left( \frac{1}{P_\parallel^6} + \frac{4p_3^2}{P_\parallel^8} + \frac{4p_3^4}{P_\parallel^{10}} \right) c_5^2 + \frac{2p_0 p_3}{P_\parallel^6} c_2 c_3 \right. \\ & + \frac{2p_0^2 p_3}{P_\parallel^8} c_2 c_4 + \left( \frac{2p_0}{P_\parallel^6} + \frac{4p_0 p_3^2}{P_\parallel^8} \right) c_2 c_5 + \frac{2p_0 p_3^2}{P_\parallel^8} c_3 c_4 + \left( \frac{2p_3}{P_\parallel^6} + \frac{4p_3^3}{P_\parallel^8} \right) c_3 c_5 \\ & \left. + \left( \frac{2p_0 p_3}{P_\parallel^8} + \frac{4p_0 p_3^3}{P_\parallel^{10}} \right) c_4 c_5 \right], \end{aligned} \quad (\text{B4})$$

$$\begin{aligned} \not\!\!\!\sum_{\{p_0\}} \frac{b^2}{P_\parallel^2} = & c_1^2 \not\!\!\!\sum_{\{p_0\}} \left[ \frac{p_3^2}{P_\parallel^6} c_2^2 + \frac{p_0^2}{P_\parallel^6} c_3^2 + \left( \frac{1}{P_\parallel^6} + \frac{4p_3^2}{P_\parallel^8} + \frac{4p_3^4}{P_\parallel^{10}} \right) c_4^2 + \frac{16p_0^2 p_3^2}{P_\parallel^{10}} c_5^2 + \frac{2p_0 p_3}{P_\parallel^6} c_2 c_3 \right. \\ & - \left( \frac{2p_3}{P_\parallel^6} + \frac{4p_3^3}{P_\parallel^8} \right) c_2 c_4 - \frac{8p_0 p_3^2}{P_\parallel^8} c_2 c_5 - \left( \frac{2p_0}{P_\parallel^6} + \frac{4p_0 p_3^2}{P_\parallel^8} \right) c_3 c_4 - \frac{8p_0^2 p_3}{P_\parallel^8} c_3 c_5 \end{aligned}$$

$$+ \left( \frac{8p_0 p_3}{P_{\parallel}^8} + \frac{16p_0 p_3^3}{P_{\parallel}^{10}} \right) c_4 c_5 \Big], \quad (\text{B5})$$

$$\begin{aligned} \sum_{\{p_0\}} \frac{a^2 p_3^2}{P_{\parallel}^4} = & c_1^2 \sum_{\{p_0\}} \left[ \frac{p_0^2 p_3^2}{P_{\parallel}^8} c_2^2 + \frac{p_3^4}{P_{\parallel}^8} c_2^2 + \frac{p_0^2 p_3^4}{P_{\parallel}^{12}} c_2^2 + \left( \frac{p_3^2}{P_{\parallel}^8} + \frac{4p_3^4}{P_{\parallel}^{10}} + \frac{4p_3^6}{P_{\parallel}^{12}} \right) c_5^2 + \frac{2p_0 p_3^3}{P_{\parallel}^8} c_2 c_3 \right. \\ & + \frac{2p_0^2 p_3^3}{P_{\parallel}^{10}} c_2 c_4 + \left( \frac{2p_0 p_3^2}{P_{\parallel}^8} + \frac{4p_0 p_3^4}{P_{\parallel}^{10}} \right) c_2 c_5 + \frac{2p_0 p_3^4}{P_{\parallel}^{10}} c_3 c_4 + \left( \frac{2p_3^3}{P_{\parallel}^8} + \frac{4p_3^5}{P_{\parallel}^{10}} \right) c_3 c_5 \\ & \left. + \left( \frac{2p_0 p_3^3}{P_{\parallel}^{10}} + \frac{4p_0 p_3^5}{P_{\parallel}^{12}} \right) c_4 c_5 \right], \quad (\text{B6}) \end{aligned}$$

$$\begin{aligned} \sum_{\{p_0\}} \frac{b^2 p_3^2}{P_{\parallel}^4} = & c_1^2 \sum_{\{p_0\}} \left[ \frac{p_3^4}{P_{\parallel}^8} c_2^2 + \frac{p_0^2 p_3^2}{P_{\parallel}^8} c_2^2 + \left( \frac{p_3^2}{P_{\parallel}^8} + \frac{4p_3^4}{P_{\parallel}^{10}} + \frac{4p_3^6}{P_{\parallel}^{12}} \right) c_4^2 + \frac{16p_0^2 p_3^4}{P_{\parallel}^{12}} c_5^2 + \frac{2p_0 p_3^3}{P_{\parallel}^8} c_2 c_3 \right. \\ & - \left( \frac{2p_3^3}{P_{\parallel}^8} + \frac{4p_3^5}{P_{\parallel}^{10}} \right) c_2 c_4 - \frac{8p_0 p_3^4}{P_{\parallel}^{10}} c_2 c_5 - \left( \frac{2p_0 p_3^2}{P_{\parallel}^8} + \frac{4p_0 p_3^4}{P_{\parallel}^{10}} \right) c_3 c_4 - \frac{8p_0^2 p_3^3}{P_{\parallel}^{10}} c_3 c_5 \\ & \left. + \left( \frac{8p_0 p_3^3}{P_{\parallel}^{10}} + \frac{16p_0 p_3^5}{P_{\parallel}^{12}} \right) c_4 c_5 \right], \quad (\text{B7}) \end{aligned}$$

$$\begin{aligned} \sum_{\{p_0\}} \frac{ab p_0 p_3}{P_{\parallel}^4} = & c_1^2 \sum_{\{p_0\}} \left[ -\frac{p_0^2 p_3^2}{P_{\parallel}^8} c_2^2 - \frac{p_0^2 p_3^2}{P_{\parallel}^8} c_3^2 + \left( \frac{p_0^2 p_3^2}{P_{\parallel}^{10}} + \frac{2p_0^2 p_3^4}{P_{\parallel}^{12}} \right) c_4^2 + \left( \frac{4p_0^2 p_3^2}{P_{\parallel}^{10}} + \frac{8p_0^2 p_3^4}{P_{\parallel}^{12}} \right) c_5^2 \right. \\ & - \left( \frac{p_0^3 p_3}{P_{\parallel}^8} + \frac{p_0 p_3^3}{P_{\parallel}^8} \right) c_2 c_3 + \left( \frac{p_0^2 p_3}{P_{\parallel}^8} + \frac{p_0^2 p_3^3}{P_{\parallel}^{10}} \right) c_2 c_4 + \left( \frac{4p_0^3 p_3^2}{P_{\parallel}^{10}} - \frac{p_0 p_3^2}{P_{\parallel}^8} - \frac{2p_0 p_3^4}{P_{\parallel}^{10}} \right) c_2 c_5 \\ & + \left( \frac{p_0 p_3^2}{P_{\parallel}^8} - \frac{p_0^3 p_3^2}{P_{\parallel}^{10}} + \frac{2p_0 p_3^4}{P_{\parallel}^{10}} \right) c_3 c_4 + \left( \frac{2p_0^2 p_3^3}{P_{\parallel}^{10}} - \frac{p_0^2 p_3}{P_{\parallel}^8} \right) c_3 c_5 \\ & \left. + \left( \frac{p_0 p_3}{P_{\parallel}^8} + \frac{4p_0 p_3^3}{P_{\parallel}^{10}} + \frac{p_0^3 p_3^3}{P_{\parallel}^{12}} + \frac{4p_0 p_3^5}{P_{\parallel}^{12}} \right) c_4 c_5 \right], \quad (\text{B8}) \end{aligned}$$

which leads to

$$\begin{aligned} F'_q = & -4d_F \sum_f \frac{q_f B}{(2\pi)^2} \sum_{\{p_0\}} \left[ \frac{c_1 c_2}{P_{\parallel}^2} + \left( \frac{2p_3}{P_{\parallel}^4} + \frac{3p_3^3}{P_{\parallel}^6} \right) c_1 c_4 + \left( \frac{p_0}{P_{\parallel}^4} + \frac{6p_0 p_3^2}{P_{\parallel}^6} \right) c_1 c_5 - \frac{c_1^2 c_2^2}{P_{\parallel}^4} - \frac{c_1^2 c_3^2}{P_{\parallel}^4} \right. \\ & - \left( \frac{1}{P_{\parallel}^6} + \frac{11p_3^2}{P_{\parallel}^8} + \frac{27p_3^4}{P_{\parallel}^{10}} + \frac{18p_3^6}{P_{\parallel}^{12}} \right) c_1^2 c_4^2 - \left( \frac{1}{P_{\parallel}^6} + \frac{38p_3^2}{P_{\parallel}^8} + \frac{108p_3^4}{P_{\parallel}^{10}} + \frac{72p_3^6}{P_{\parallel}^{12}} \right) c_1^2 c_5^2 \\ & - \left( \frac{4p_3}{P_{\parallel}^6} + \frac{6p_3^3}{P_{\parallel}^8} \right) c_1^2 c_2 c_4 - \left( \frac{2p_0}{P_{\parallel}^6} + \frac{12p_0 p_3^2}{P_{\parallel}^8} \right) c_1^2 c_2 c_5 + \left( \frac{2p_0}{P_{\parallel}^6} + \frac{6p_0 p_3^2}{P_{\parallel}^8} \right) c_1^2 c_3 c_4 \\ & \left. + \left( \frac{10p_3}{P_{\parallel}^6} + \frac{12p_3^3}{P_{\parallel}^8} \right) c_1^2 c_3 c_5 - \left( \frac{14p_0 p_3}{P_{\parallel}^8} + \frac{72p_0 p_3^3}{P_{\parallel}^{10}} + \frac{72p_0 p_3^5}{P_{\parallel}^{12}} \right) c_1^2 c_4 c_5 \right] \\ = & -4d_F \sum_f \frac{q_f B}{(2\pi)^2} \sum_{\{p_0\}} \left[ \frac{c_1 c_2}{P_{\parallel}^2} - \frac{c_1^2 c_2^2}{P_{\parallel}^4} - \frac{c_1^2 c_3^2}{P_{\parallel}^4} - \left( \frac{1}{P_{\parallel}^6} + \frac{11p_3^2}{P_{\parallel}^8} + \frac{27p_3^4}{P_{\parallel}^{10}} + \frac{18p_3^6}{P_{\parallel}^{12}} \right) c_1^2 c_4^2 \right. \\ & \left. - \left( \frac{1}{P_{\parallel}^6} + \frac{38p_3^2}{P_{\parallel}^8} + \frac{108p_3^4}{P_{\parallel}^{10}} + \frac{72p_3^6}{P_{\parallel}^{12}} \right) c_1^2 c_5^2 \right]. \quad (\text{B9}) \end{aligned}$$

One can calculate the Matsubara frequency sum as [81]

$$\sum_{\{p_0\}} \frac{1}{P_{\parallel}^2} = -\frac{1}{2p_3} \left( 1 - n_F(p_3 + \mu) - n_F(p_3 - \mu) \right), \quad (\text{B10})$$

The first term in Eq. (B10) is temperature independent vacuum term and can be regularized using regular vacuum regularization. The regularized contribution will be temperature independent and will not contribute anything to the thermodynamics of the system. So, without vacuum term, Eq. (B10) becomes

$$\sum_{\{p_0\}} \frac{1}{P_{||}^2} = \frac{1}{2p_3} \left( n_F(p_3 + \mu) + n_F(p_3 - \mu) \right). \quad (\text{B11})$$

Now one can write the sum-integral as

$$\not\sum_{\{p_0\}} \frac{1}{P_{||}^2} = \left( \frac{e^{\gamma_E} \Lambda^2}{4\pi} \right)^\epsilon \int_{-\infty}^{\infty} \frac{d^{1-2\epsilon} p_3}{2p_3} \left( n_F(p_3 + \mu) + n_F(p_3 - \mu) \right). \quad (\text{B12})$$

We perform the sum-integrals [53] in Eq. (B9) as

$$\begin{aligned} \not\sum_{\{p_0\}} \frac{1}{P_{||}^2} &= \left( \frac{e^{\gamma_E} \Lambda^2}{4\pi} \right)^\epsilon \int_{-\infty}^{\infty} d^{1-2\epsilon} p_3 \frac{n_F(p_3)}{p_3} \\ &= \left( \frac{\Lambda}{4\pi T} \right)^{2\epsilon} \left[ -\frac{1}{2\epsilon} - \frac{1}{2} (3\gamma_E + 4\ln 2 - \ln \pi) + \frac{7\mu^2 \zeta(3)}{4\pi^2 T^2} - \frac{31\mu^4 \zeta(5)}{16\pi^4 T^4} + \mathcal{O}(\epsilon) \right], \end{aligned} \quad (\text{B13})$$

$$\not\sum_{\{p_0\}} \frac{1}{P_{||}^4} = \left( \frac{\Lambda}{4\pi T} \right)^{2\epsilon} \left[ \frac{7}{8\pi^2} \frac{\zeta(3)}{T^2} - \frac{93\mu^2 \zeta(5)}{16\pi^4 T^4} 31 + \frac{1905\mu^4 \zeta(7)}{128\pi^6 T^6} + \mathcal{O}(\epsilon) \right], \quad (\text{B14})$$

$$\not\sum_{\{p_0\}} \frac{1}{P_{||}^6} = \left( \frac{\Lambda}{4\pi T} \right)^{2\epsilon} \left[ -\frac{93\zeta(5)}{128\pi^4 T^4} + \frac{5715\mu^2 \zeta(7)}{512\pi^6 T^6} - \frac{53655\mu^4 \zeta(9)}{1024\pi^8 T^8} + \mathcal{O}(\epsilon) \right], \quad (\text{B15})$$

$$\not\sum_{\{p_0\}} \frac{p_3^2}{P_{||}^8} = \left( \frac{\Lambda}{4\pi T} \right)^{2\epsilon} \left[ \frac{31\zeta(5)}{256\pi^4 T^4} - \frac{1905\mu^2 \zeta(7)}{1024\pi^6 T^6} + \frac{17885\mu^4 \zeta(9)}{2048\pi^8 T^8} + \mathcal{O}(\epsilon) \right], \quad (\text{B16})$$

$$\not\sum_{\{p_0\}} \frac{p_3^4}{P_{||}^{10}} = \left( \frac{\Lambda}{4\pi T} \right)^{2\epsilon} \left[ -\frac{93\zeta(5)}{2048\pi^4 T^4} 31 + \frac{5715\mu^2 \zeta(7)}{8192\pi^6 T^6} - \frac{53655\mu^4 \zeta(9)}{16384\pi^8 T^8} + \mathcal{O}(\epsilon) \right], \quad (\text{B17})$$

$$\not\sum_{\{p_0\}} \frac{p_3^6}{P_{||}^{12}} = \left( \frac{\Lambda}{4\pi T} \right)^{2\epsilon} \left[ \frac{93\zeta(5)}{4096\pi^4 T^4} - \frac{5715\mu^2 \zeta(7)}{16384\pi^6 T^6} + \frac{53655\mu^4 \zeta(9)}{32768\pi^8 T^8} + \mathcal{O}(\epsilon) \right], \quad (\text{B18})$$

where  $\Lambda$  is the  $\overline{\text{MS}}$  renormalization scale.

Using the above sum-integrals in Eq. (B9)  $F'_q$  up to  $\mathcal{O}(g^4)$  becomes,

$$\begin{aligned} F'_q &= -4d_F \sum_f \frac{q_f B}{(2\pi)^2} \not\sum_{\{p_0\}} \left[ \frac{c_1 c_2}{P_{||}^2} - \frac{c_1^2 c_2^2}{P_{||}^4} - \frac{c_1^2 c_3^2}{P_{||}^4} - \left( \frac{1}{P_{||}^6} + \frac{11p_3^2}{P_{||}^8} + \frac{27p_3^4}{P_{||}^{10}} + \frac{18p_3^6}{P_{||}^{12}} \right) c_1^2 c_4^2 \right. \\ &\quad \left. - \left( \frac{1}{P_{||}^6} + \frac{38p_3^2}{P_{||}^8} + \frac{108p_3^4}{P_{||}^{10}} + \frac{72p_3^6}{P_{||}^{12}} \right) c_1^2 c_5^2 \right] \end{aligned}$$

$$\begin{aligned}
&= 4d_F \sum_f \frac{q_f B}{(2\pi)^2} \frac{g^2 C_F(q_f B)}{4\pi^2} \left( \frac{\Lambda}{4\pi T} \right)^{2\epsilon} \left[ \frac{1}{\epsilon} \left( -\frac{1}{2} \ln 2 + \frac{7\mu^2 \zeta(3)}{16\pi^2 T^2} - \frac{31\mu^4 \zeta(5)}{64\pi^4 T^4} \right) - \frac{3\gamma_E \ln 2}{2} \right. \\
&+ \ln 2 \ln \pi - \frac{1}{2} \ln 2 \ln 16\pi + \frac{g^2 C_F(q_f B)}{4\pi^2} \frac{63 \ln^2 \zeta(3)}{72\pi^2 T^2} - \frac{g^2 C_F(q_f B)}{4\pi^2} \frac{217(q_f B)^2 \zeta(5)}{36864\pi^4 T^6} \\
&\times \left( \gamma_E + 2 \ln 2 - 12 \ln G \right)^2 + \frac{\mu^2}{1152\pi^2 T^4} \left\{ \frac{7\zeta(3)g^2 C_F(q_f B)}{4\pi^2} \left( 3 + 3\gamma_E + 4 \ln 2 - 36 \ln G \right)^2 \right. \\
&+ 504T^2 \zeta(3) \left( 3\gamma_E + 8 \ln 2 - \ln \pi \right) - \frac{36 \ln 2}{\pi^2} \frac{g^2 C_F(q_f B)}{4\pi^2} \left( 49\zeta(3)^2 + 186 \ln 2 \zeta(5) \right) \Big\} \\
&- \frac{7(q_f B)^2 \mu^2}{737280\pi^4 T^8} \frac{g^2 C_F(q_f B)}{4\pi^2} \left\{ -31\zeta(5) \left( -15 + 15\gamma_E + 16 \ln 2 \right) \left( \gamma_E + 2 \ln 2 - 12 \ln G \right) \right. \\
&- \frac{48825}{\pi^4} \zeta(3)^2 \zeta(5) - \frac{9525\zeta(7)}{\pi^2} \left( \gamma_E + 2 \ln 2 - 12 \ln G \right)^2 + 55800\zeta(5)\zeta'(-3) \\
&\times \left( \gamma_E + 2 \ln 2 - 12 \ln G \right) \Big\} + \frac{\mu^4}{69120\pi^6 T^6} \left\{ -1080\pi^2 T^2 \left( 98\zeta(3)^2 + 31\zeta(5) \left( 3\gamma_E + 8 \ln 2 - \ln \pi \right) \right) \right. \\
&- \frac{g^2 C_F(q_f B)}{4\pi^2} \left( 14\pi^4 \zeta(3) \left( 15\gamma_E + 16 \ln 2 \right) \left( 3 + 3\gamma_E + 4 \ln 2 - 36 \ln G \right) - 46305\zeta(3)^3 \right. \\
&+ 2790\pi^2 \zeta(5) \left( 3 + 3\gamma_E - 4 \ln 2 - 36 \ln G \right)^2 - 820260 \ln 2 \zeta(3) \zeta(5) - 1028700 \ln^2 \zeta(7) \\
&- 25200\pi^4 \zeta(3) \zeta'(-3) \left( 3 + 3\gamma_E + 4 \ln 2 - 36 \ln G \right) \Big\} - \frac{\mu^4 (q_f B)^2}{5308416\pi^4 T^{10}} \frac{g^2 C_F(q_f B)}{4\pi^2} \\
&\times \left\{ \frac{10897740}{\pi^6} \zeta(3) \zeta(5)^2 + \frac{37804725}{\pi^6} \zeta(3)^2 \zeta(7) + \frac{2253510\zeta(9)}{\pi^4} \left( \gamma_E + 2 \ln 2 - 12 \ln G \right)^2 \right. \\
&+ \frac{24003}{\pi^2} \zeta(7) \left( \gamma_E + 2 \ln 2 - 12 \ln G \right) \left( -15 + 15\gamma_E + 16 \ln 2 - 1800\zeta'(-3) \right) \\
&+ \frac{31\zeta(5)}{100} \left( 14175 - 40950\gamma_E + 26775\gamma_E^2 + 68240\gamma_E \ln 2 + 41728 \ln^2 2 + 151200 \ln G \right. \\
&- 151200\gamma_E \ln G - 240 \ln 2 \left( 231 + 640 \ln G \right) + 3175200\zeta'(-5) \left( \gamma_E + 2 \ln 2 - 12 \ln G \right) \\
&- 226800\zeta'(-3) \left( -15 + 15\gamma_E + 16 \ln 2 \right) + 204120000\zeta'(-3)^2 \Big\} \Big] \quad (B19)
\end{aligned}$$

- 
- [1] S. Jeon and V. Koch, “Charged particle ratio fluctuation as a signal for QGP,” Phys. Rev. Lett. **85**, 2076-2079 (2000).
- [2] M. Asakawa, U. W. Heinz and B. Muller, “Fluctuation probes of quark deconfinement,” Phys. Rev. Lett. **85**, 2072-2075 (2000).
- [3] V. Koch, M. Bleicher and S. Jeon, “Event-by-event fluctuations and the QGP,” Nucl. Phys. A **698**, 261-268 (2002).
- [4] R. Bellwied, S. Borsanyi, Z. Fodor, S. Katz, A. Pasztor, C. Ratti and K. Szabo, “Fluctuations and correlations in high temperature QCD,” Phys. Rev. D **92**, no.11, 114505 (2015).

- [5] S. Borsanyi, Z. Fodor, S. Katz, S. Krieg, C. Ratti and K. Szabo, “Freeze-out parameters: lattice meets experiment,” *Phys. Rev. Lett.* **111**, 062005 (2013).
- [6] S. Borsanyi, “Thermodynamics of the QCD transition from lattice,” *Nucl. Phys. A* **904-905**, 270c-277c (2013).
- [7] H. T. Ding, S. Mukherjee, H. Ohno, P. Petreczky and H. P. Schadler, “Diagonal and off-diagonal quark number susceptibilities at high temperatures,” *Phys. Rev. D* **92**, no.7, 074043 (2015).
- [8] R. Gavai and S. Gupta, “Fluctuations, strangeness and quasi-quarks in heavy-ion collisions from lattice QCD,” *Phys. Rev. D* **73**, 014004 (2006).
- [9] N. Haque, A. Bandyopadhyay, J. O. Andersen, M. G. Mustafa, M. Strickland and N. Su, “Three-loop HTLpt thermodynamics at finite temperature and chemical potential,” *JHEP* **05** (2014), 027.
- [10] N. Haque, J. O. Andersen, M. G. Mustafa, M. Strickland and N. Su, “Three-loop pressure and susceptibility at finite temperature and density from hard-thermal-loop perturbation theory,” *Phys. Rev. D* **89** (2014) no.6, 061701.
- [11] N. Haque, M. G. Mustafa and M. Strickland, “Quark Number Susceptibilities from Two-Loop Hard Thermal Loop Perturbation Theory,” *JHEP* **07** (2013), 184.
- [12] P. Chakraborty, M. G. Mustafa and M. H. Thoma, “Quark number susceptibility, thermodynamic sum rule, and hard thermal loop approximation,” *Phys. Rev. D* **68** (2003), 085012.
- [13] P. Chakraborty, M. G. Mustafa and M. H. Thoma, “Quark number susceptibility in hard thermal loop approximation,” *Eur. Phys. J. C* **23** (2002), 591-596.
- [14] J. Blaizot, E. Iancu and A. Rebhan, “Quark number susceptibilities from HTL resummed thermodynamics,” *Phys. Lett. B* **523** (2001), 143-150.
- [15] A. Vuorinen, “Quark number susceptibilities of hot QCD up to  $g^6 \ln g$ ,” *Phys. Rev. D* **67** (2003), 074032.
- [16] T. Toimela, “Perturbative QED and QCD at Finite Temperatures and Densities,” *Int. J. Theor. Phys.* **24** (1985), 901.
- [17] A. Vuorinen, “The Pressure of QCD at finite temperatures and chemical potentials,” *Phys. Rev. D* **68** (2003), 054017.
- [18] N. Haque, “Quark mass dependent collective excitations and quark number susceptibilities within the hard thermal loop approximation,” *Phys. Rev. D* **98** (2018) no.1, 014013.
- [19] V. Skokov, A. Illarionov and V. Toneev, “Estimate of the magnetic field strength in heavy-ion collisions,” *Int. J. Mod. Phys. A* **24** (2009), 5925-5932.
- [20] D. E. Kharzeev, L. D. McLerran and H. J. Warringa, “The Effects of topological charge change in heavy ion collisions: ‘Event by event P and CP violation’,” *Nucl. Phys. A* **803** (2008), 227-253.
- [21] I. A. Shovkovy, “Magnetic Catalysis: A Review,” *Lect. Notes Phys.* **871** (2013), 13-49.
- [22] M. D’Elia, “Lattice QCD Simulations in External Background Fields,” *Lect. Notes Phys.* **871** (2013), 181-208.
- [23] K. Fukushima, “Views of the Chiral Magnetic Effect,” *Lect. Notes Phys.* **871** (2013), 241-259.
- [24] N. Mueller, J. A. Bonnet and C. S. Fischer, “Dynamical quark mass generation in a strong external

- magnetic field,” *Phys. Rev. D* **89** (2014) no.9, 094023.
- [25] V. A. Miransky and I. A. Shovkovy, “Quantum field theory in a magnetic field: From quantum chromodynamics to graphene and Dirac semimetals,” *Phys. Rept.* **576** (2015), 1-209.
  - [26] V. Gusynin, V. Miransky and I. Shovkovy, “Dimensional reduction and dynamical chiral symmetry breaking by a magnetic field in (3+1)-dimensions,” *Phys. Lett. B* **349** (1995), 477-483.
  - [27] V. Gusynin, V. Miransky and I. Shovkovy, “Dynamical chiral symmetry breaking by a magnetic field in QED,” *Phys. Rev. D* **52** (1995), 4747-4751.
  - [28] G. Bali, F. Bruckmann, G. Endrodi, Z. Fodor, S. Katz, S. Krieg, A. Schafer and K. Szabo, “The QCD phase diagram for external magnetic fields,” *JHEP* **02** (2012), 044.
  - [29] A. Ayala, C. Dominguez, L. Hernandez, M. Loewe and R. Zamora, “Inverse magnetic catalysis from the properties of the QCD coupling in a magnetic field,” *Phys. Lett. B* **759** (2016), 99-103.
  - [30] A. Ayala, M. Loewe, A. J. Mizher and R. Zamora, “Inverse magnetic catalysis for the chiral transition induced by thermo-magnetic effects on the coupling constant,” *Phys. Rev. D* **90** (2014), 036001.
  - [31] A. Ayala, M. Loewe and R. Zamora, “Inverse magnetic catalysis in the linear sigma model with quarks,” *Phys. Rev. D* **91** (2015), 016002.
  - [32] F. Bruckmann, G. Endrodi and T. G. Kovacs, “Inverse magnetic catalysis and the Polyakov loop,” *JHEP* **1304**, 112 (2013).
  - [33] R. L. S. Farias, V. S. Timoteo, S. S. Avancini, M. B. Pinto and G. Krein, “Thermo-magnetic effects in quark matter: Nambu–Jona-Lasinio model constrained by lattice QCD,” *Eur. Phys. J. A* **53**, 101 (2017) doi:10.1140/epja/i2017-12320-8.
  - [34] R. L. S. Farias, K. P. Gomes, G. I. Krein and M. B. Pinto, “Importance of asymptotic freedom for the pseudocritical temperature in magnetized quark matter,” *Phys. Rev. C* **90**, 025203 (2014) doi:10.1103/PhysRevC.90.025203.
  - [35] M. Ferreira, P. Costa, O. Lourenço, T. Frederico and C. Providência, “Inverse magnetic catalysis in the (2+1)-flavor Nambu–Jona-Lasinio and Polyakov–Nambu–Jona-Lasinio models,” *Phys. Rev. D* **89**, 116011 (2014).
  - [36] N. Mueller and J. M. Pawłowski, “Magnetic catalysis and inverse magnetic catalysis in QCD,” *Phys. Rev. D* **91**, 116010 (2015).
  - [37] K. Fukushima, D. E. Kharzeev and H. J. Warringa, “The Chiral Magnetic Effect,” *Phys. Rev. D* **78** (2008), 074033.
  - [38] D. E. Kharzeev, “The Chiral Magnetic Effect and Anomaly-Induced Transport,” *Prog. Part. Nucl. Phys.* **75** (2014), 133-151.
  - [39] G. S. Bali, B. B. Brandt, G. Endrődi and B. Gläsel, “Meson masses in electromagnetic fields with Wilson fermions,” *Phys. Rev. D* **97** (2018) no.3, 034505.
  - [40] A. Ayala, R. L. Farias, S. Hernández-Ortiz, L. Hernández, D. M. Paret and R. Zamora, “Magnetic field-dependence of the neutral pion mass in the linear sigma model coupled to quarks: The weak field case,” *Phys. Rev. D* **98** (2018) no.11, 114008.

- [41] A. Das and N. Haque, “Neutral pion mass in the linear sigma model coupled to quarks at arbitrary magnetic field,” *Phys. Rev. D* **101** (2020) no.7, 074033.
- [42] S. Fayazbakhsh, S. Sadeghian and N. Sadooghi, “Properties of neutral mesons in a hot and magnetized quark matter,” *Phys. Rev. D* **86**, 085042 (2012).
- [43] M. Coppola, D. Gómez Dumm and N. N. Scoccola, “*Charged pion masses under strong magnetic fields in the NJL model*,” *Phys. Lett. B* **782**, 155 (2018).
- [44] D. Gómez Dumm, M. F. Izzo Villafañe and N. N. Scoccola, “*Phys. Rev. D* **97**, no. 3, 034025 (2018).
- [45] S. S. Avancini, W. R. Tavares and M. B. Pinto, “Properties of magnetized neutral mesons within a full RPA evaluation,” *Phys. Rev. D* **93**, no. 1, 014010 (2016).
- [46] R. Zhang, W. j. Fu and Y. x. Liu, “Properties of Mesons in a Strong Magnetic Field,” *Eur. Phys. J. C* **76**, no. 6, 307 (2016).
- [47] S. S. Avancini, R. L. S. Farias and W. R. Tavares, “*Neutral meson properties in hot and magnetized quark matter: a new magnetic field independent regularization scheme applied to NJL-type model*,” *Phys. Rev. D* **99**, no. 5, 056009 (2019).
- [48] S. S. Avancini, R. L. S. Farias, M. Benghi Pinto, W. R. Tavares and V. S. Timóteo, “ *$\pi_0$  pole mass calculation in a strong magnetic field and lattice constraints*,” *Phys. Lett. B* **767**, 247 (2017).
- [49] H. Liu, X. Wang, L. Yu and M. Huang, “Neutral and charged scalar mesons, pseudoscalar mesons, and diquarks in magnetic fields,” *Phys. Rev. D* **97**, no.7, 076008 (2018).
- [50] H. Liu, L. Yu and M. Huang, “Charged and neutral vector  $\rho$  mesons in a magnetic field,” *Phys. Rev. D* **91**, no.1, 014017 (2015).
- [51] H. Liu, L. Yu, M. Chernodub and M. Huang, “Possible formation of high temperature superconductor at an early stage of heavy-ion collisions,” *Phys. Rev. D* **94**, no.11, 113006 (2016).
- [52] M. N. Chernodub, “Spontaneous electromagnetic superconductivity of vacuum in strong magnetic field: evidence from the Nambu–Jona-Lasinio model,” *Phys. Rev. Lett.* **106**, 142003 (2011).
- [53] B. Karmakar, R. Ghosh, A. Bandyopadhyay, N. Haque and M. G. Mustafa, “Anisotropic pressure of deconfined QCD matter in presence of strong magnetic field within one-loop approximation,” *Phys. Rev. D* **99** (2019) no.9, 094002.
- [54] A. Bandyopadhyay, B. Karmakar, N. Haque and M. G. Mustafa, “Pressure of a weakly magnetized hot and dense deconfined QCD matter in one-loop hard-thermal-loop perturbation theory,” *Phys. Rev. D* **100** (2019) no.3, 034031.
- [55] M. Kurian and V. Chandra, “Bulk viscosity of a hot QCD medium in a strong magnetic field within the relaxation-time approximation,” *Phys. Rev. D* **97** (2018) no.11, 116008.
- [56] M. Kurian and V. Chandra, “Effective description of hot QCD medium in strong magnetic field and longitudinal conductivity,” *Phys. Rev. D* **96** (2017) no.11, 114026.
- [57] A. Das, N. Haque, M. G. Mustafa and P. K. Roy, “Hard dilepton production from a weakly magnetized hot QCD medium,” *Phys. Rev. D* **99** (2019) no.9, 094022.
- [58] A. Bandyopadhyay, C. A. Islam and M. G. Mustafa, “Electromagnetic spectral properties and Debye

- screening of a strongly magnetized hot medium,” *Phys. Rev. D* **94** (2016) no.11, 114034.
- [59] A. Bandyopadhyay and S. Mallik, “Effect of magnetic field on dilepton production in a hot plasma,” *Phys. Rev. D* **95** (2017) no.7, 074019.
  - [60] T. K. Chyi, C. W. Hwang, W. Kao, G. L. Lin, K. W. Ng and J. J. Tseng, “The weak field expansion for processes in a homogeneous background magnetic field,” *Phys. Rev. D* **62** (2000), 105014.
  - [61] K. Tuchin, “Magnetic contribution to dilepton production in heavy-ion collisions,” *Phys. Rev. C* **88** (2013), 024910.
  - [62] S. Ghosh and V. Chandra, “Electromagnetic spectral function and dilepton rate in a hot magnetized QCD medium,” *Phys. Rev. D* **98** (2018) no.7, 076006.
  - [63] A. Bzdak and V. Skokov, “Anisotropy of photon production: initial eccentricity or magnetic field,” *Phys. Rev. Lett.* **110** (2013) no.19, 192301.
  - [64] G. Basar, D. Kharzeev, D. Kharzeev and V. Skokov, “Conformal anomaly as a source of soft photons in heavy ion collisions,” *Phys. Rev. Lett.* **109** (2012), 202303.
  - [65] R. Ghosh, B. Karmakar and M. G. Mustafa, “Soft contribution to the damping rate of a hard photon in a weakly magnetized hot medium,” *Phys. Rev. D* **101** (2020) no.5, 056007.
  - [66] A. Bzdak and V. Skokov, “Event-by-event fluctuations of magnetic and electric fields in heavy ion collisions,” *Phys. Lett. B* **710** (2012), 171-174.
  - [67] L. McLerran and V. Skokov, “Comments About the Electromagnetic Field in Heavy-Ion Collisions,” *Nucl. Phys. A* **929** (2014), 184-190.
  - [68] K. Tuchin, “Electromagnetic radiation by quark-gluon plasma in a magnetic field,” *Phys. Rev. C* **87** (2013) no.2, 024912.
  - [69] K. Tuchin, “Particle production in strong electromagnetic fields in relativistic heavy-ion collisions,” *Adv. High Energy Phys.* **2013** (2013), 490495.
  - [70] K. Tuchin, “Time and space dependence of the electromagnetic field in relativistic heavy-ion collisions,” *Phys. Rev. C* **88** (2013) no.2, 024911.
  - [71] T. Steinert and W. Cassing, “Electric and magnetic response of hot QCD matter,” *Phys. Rev. C* **89**, no. 3, 035203 (2014).
  - [72] K. Hattori and D. Satow, “Electrical Conductivity of Quark-Gluon Plasma in Strong Magnetic Fields,” *Phys. Rev. D* **94**, no. 11, 114032 (2016).
  - [73] S. Ghosh, A. Bandyopadhyay, R. L. S. Farias, J. Dey and G. Krein, “Anisotropic electrical conductivity of magnetized hot quark matter,” [arXiv:1911.10005 [hep-ph]].
  - [74] K. Fukushima and Y. Hidaka, “Electric conductivity of hot and dense quark matter in a magnetic field with Landau level resummation via kinetic equations,” *Phys. Rev. Lett.* **120**, no. 16, 162301 (2018).
  - [75] M. Strickland, V. Dexheimer and D. Menezes, “Bulk Properties of a Fermi Gas in a Magnetic Field,” *Phys. Rev. D* **86** (2012), 125032.
  - [76] B. Karmakar, A. Bandyopadhyay, N. Haque and M. G. Mustafa, “General structure of gauge boson propagator and its spectra in a hot magnetized medium,” *Eur. Phys. J. C* **79** (2019) no.8, 658.

- [77] A. Ayala, C. A. Dominguez, S. Hernandez-Ortiz, L. A. Hernandez, M. Loewe, D. Manreza Paret and R. Zamora, “Thermomagnetic evolution of the QCD strong coupling,” *Phys. Rev. D* **98**, no.3, 031501 (2018).
- [78] J. Beringer *et al.* [Particle Data Group], “Review of Particle Physics (RPP),” *Phys. Rev. D* **86**, 010001 (2012).
- [79] A. Perez Martinez, H. Perez Rojas and H. Mosquera Cuesta, “Anisotropic Pressures in Very Dense Magnetized Matter,” *Int. J. Mod. Phys. D* **17** (2008), 2107-2123.
- [80] G. Bali, F. Bruckmann, G. Endrödi, S. Katz and A. Schäfer, “The QCD equation of state in background magnetic fields,” *JHEP* **08**, 177 (2014).
- [81] M. L. Bellac, *Thermal Field Theory* (Cambridge University Press, Cambridge, England, 1996).